# Computational Methods for Tension Structures

**Session Organizer:** SeungDoeg KIM (Semyung University)

**Keynote Lecture**
On the development of general purpose computational program for nonlinear analysis of soft/hard structures
*SeungDeog KIM (Semyung University)*

Lateral buckling load formulation for multi-strut beam string structures
*Jaeyeol KIM* (Hyupsung University), Minger WU (Tongji University)*

A simple procedure for the analysis of hyperelastic 3D membrane structures
*Vinicius F. ARCARO (UNICAMP, Brazil)*

Test on the mechanical properties of architectural membrane
*Kang-geun PARK*, Seong-kee YOON (Pusan National University), Woo-hong JEON (Korea Apparel Testing & Research Institute)*

**Keynote Lecture**
Simplified computer-aided form-finding procedures applied to lightweight structures
*Juan Gerardo OLIVA SALINAS*, Eric VALDEZ OLMEDO (UNAM)*

Shape formation of ETFE film cushion by heat and pressure considering visco-plastic characteristics
*Masaya KAWABATA*, Kaoru NISHIKAWA (Yokohama National University)*

Shape finding of membrane structures by the natural force density method
*Ruy M.O. PAULETTI*, Paulo M. PIMENTA (University of São Paulo)*

Topology and shape of tensegrity structures
*Jingyao ZHANG*, Makoto OHSAKI (Kyoto University)*

For multiple-author papers:
Contact author designated by *
Presenting author designated by underscore

Proceedings of the 6th International Conference on
Computation of Shell and Spatial Structures
IASS-IACM 2008: "Spanning Nano to Mega"
28-31 May 2008, Cornell University, Ithaca, NY, USA
John F. ABEL and J. Robert COOKE (eds.)

# On the development of general purpose computational program for nonlinear analysis of soft/hard structures

SeungDeog KIM*

*Department of Architectural Engineering, Semyung University
579 Sinweol-Dong, Jecheon, Chungbuk 390-711, Korea
sabinus@semyung.ac.kr

## Abstract

Spatial structures have to be analyzed by considering geometric nonlinearity, and the nonlinear problem is very sensitive to initial conditions. The efficiency of a computer program depends on the possibility of convergence and the speed in nonlinear procedure.

This study introduces NASS, short for Nonlinear Analysis for Spatial Structures - a new nonlinear analysis program under development. NASS, the first of its kind, is being developed for both soft and hard structures to get nonlinear solutions and to target a general purpose computational program. Using examples NASS ability in both soft and hard structures is proved.

## 1. Introduction

Structural designers use a variety of multi-purpose and commercial structural analysis computer programs to design various types of buildings. Unfortunately, in the spatial structures field we cannot find useful common programs for large-span roofs. Most companies or laboratories design spatial structures by using in-house, untested programs. This lack of public verification of the program results in potentially unsafe structures. Particularly, spatial structures need to be analyzed by considering geometric nonlinearity, and the nonlinear problem is very sensitive to initial conditions. Also the efficiency of a computer program depends on the possibility of convergence and the speed in nonlinear procedure.

In this study, I will introduce a new nonlinear analysis program NASS under development, short for Nonlinear Analysis for Spatial Structures. NASS is being developed for both soft and hard structures to get nonlinear solutions and to target a general purpose computational program for the first time. NASS has created many tools to solve various problems for spatial structures.

## 2. Functions of NASS

Nowadays there are many structural systems in large span structures using new materials. To build safer and more economical large span structures, we need more advanced, stronger and more lightweight, materials. When a new material is developed to improve some existing problems, the design method also has to be advanced for the material. This evolution gives us the spatial structures to be built more reasonably, and to be more complicated in structural systems. Therefore we have too many structural systems to classify the systems clearly.

Here I would like to propose a simple figure where various structural systems can be classified with ease, as shown in Figure 1. In this figure, first we can group into two parts according to materials. The first one is the hard structures which are made by reinforced concrete, steel frames and so on; initial structural shapes under unloading have been determined to be a fixed form. The other is the soft structures which are made by fabrics, cables and so on; initial structural shapes under unloading have not been determined. These two structural systems reveal different behaviors. In the former, structural stability changes from stable to unstable as the external load level gets higher and reaches a certain critical point. But the latter shows the opposite phenomenon,

namely from unstable to stable in an untensioned state. In structural design, therefore, the hard structures need to check the critical load due to the bucking phenomena, but the soft structures need shape finding due to the introduction of initial stresses.

Secondly, we can group the spatial structures according to how to assemble; the one is built by continuous system such as shells and membrane structures, and the other is discrete system such as space frames and space cables.

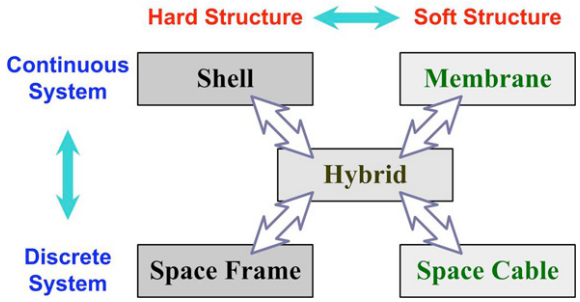


Figure 1: Classification of spatial structures

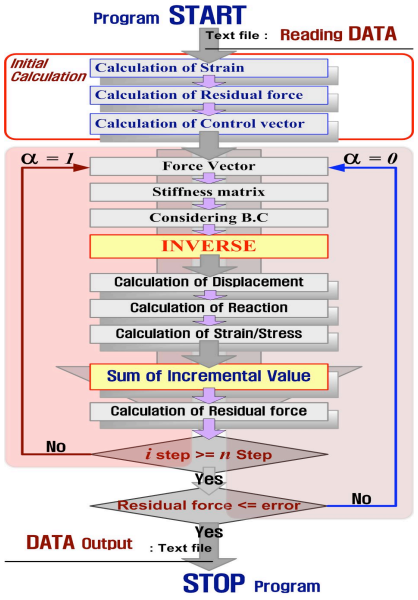


Figure 2: Flowchart of NASS

To analyze various structural systems considering geometric nonlinearity, NASS is developing many tools to solve various problems for spatial structures, as follows:

- For hard structures, such as continuum shells and space frames;
  - Getting solutions of geometric nonlinear stress-deformation analysis
  - Checking critical loads including snap-through and bifurcation
- For soft structures, such as membrane structures and space cables;
  - Getting shape finding solutions,
  - Getting solutions of geometric nonlinear stress-deformation analysis
- For construction analysis;
  - Getting erection procedure analysis for space cables
  - Getting pattern design plan for membrane structures

Some numerical schemes are used in the package for the geometric nonlinear problems, such as the Newton-Raphson method, the incremental method and so on. Users can select one or multi-schemes simultaneously from their experiences to improve the possibility of convergence and to accelerate their speed in nonlinear iteration procedure. Figure 2 shows the flowchart of NASS to explain the nonlinear procedures.

## 3. Soft structures

As an example for the design of soft structures, the Western Dome is chosen in this article, as shown in Figure 3. This elliptical cone typed dome is built by PTFE fabric, and the projected plane has 31.4m and 25m of diameters in long direction and short direct, respectively, and the height is about 9.95m to the center of upper ring. For shape analysis, the initial shape is selected like in Figure 4, and the shape after shape analysis is shown in Figure 5. From the result of shape analysis, we can find that this shape needs reinforcement by cables, because it shows the bottleneck in the upper part of the structure.

Figure 3: Western Dome

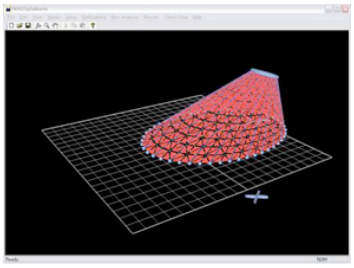

Figure 4: Initial step

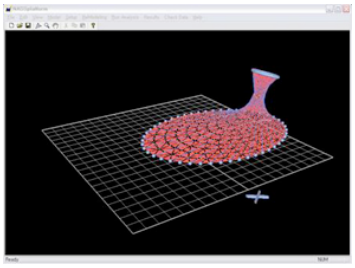

Figure 5: After shape analysis

To avoid the bottleneck, strand ropes reinforce inside the PTFE fabric, and the results show in Figure 6 and 7, which are tensed by 5tonf and 10tf tension, respectively. Figure 8 shows the compared elevation lines.

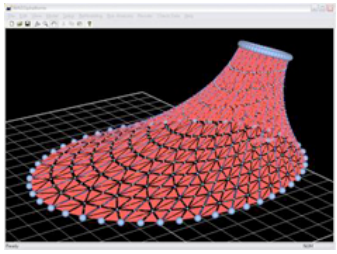

Figure 6: 5tf of tension cables

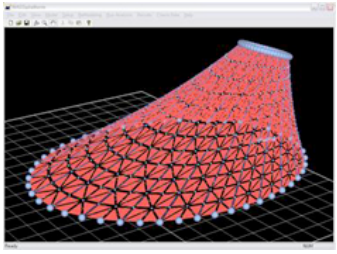

Figure 7: 10tf of tension cables

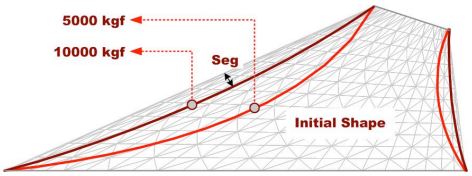


Figure 8: Comparison of shapes

After shape analysis for finding the initial shape, we can go on analyzing the nonlinear stress-deformation analysis to ensure the safety of the dome. Figure 9, 10 and 11 show the result subjected to dead load, wind-up load and wind-down load, respectively.

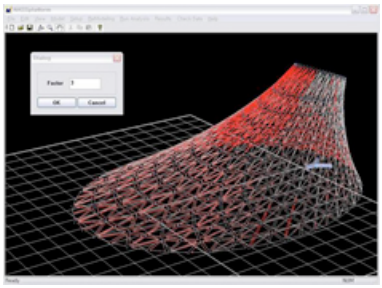

Figure 9: After dead load

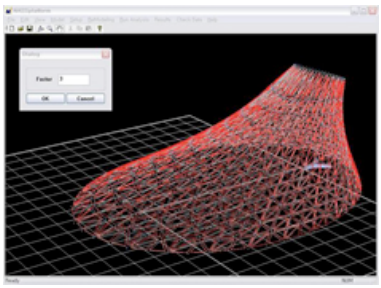

Figure 10: After wind-up load

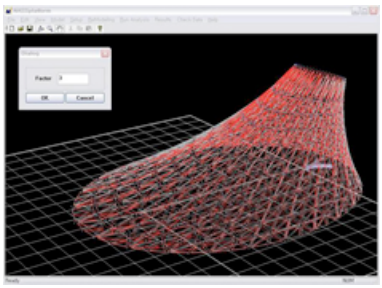

Figure 11: After wind-down load

As a special point of soft structures, we have to prepare the fabric patterns for construction. NASS offers the pattern design, and the results for pattern design and construction drawings are shown in Figure 12 and 13, respectively.

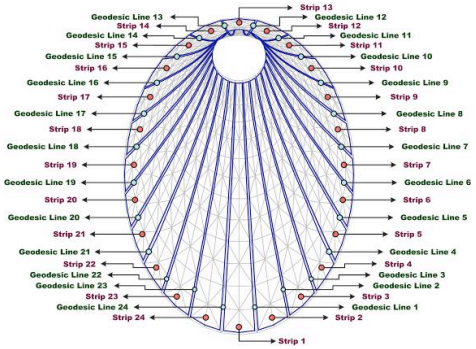


Figure 12: Pattern design

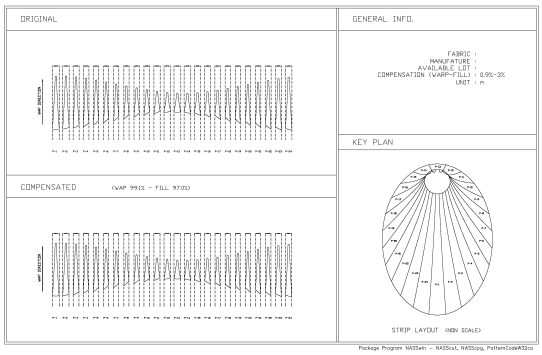


Figure 13: Construction drawings

## 4. Hard structures

For the design of hard structures, we have to check the structural instability. This is a geometric nonlinear problem, and it reveals very sensitive behavior depending on initial conditions. In shell typed roof structures, particularly, the critical load level is steeply going down according to amount of initial imperfections. The instability phenomena are classified in Figure 14.

As an example for the design of hard structures, the Speedom checks the failure load by the bifurcation, as shown in Figure 15. Diameters of the elliptical dome are 180m and 150m in long direction and short direction, respectively. Figure 16 shows skeleton of the roof and finite element meshes.

Figure 17 to 20 show the nonlinear load-displacement curves at selected nodes calculated by NASS which are under conditions of eccentric load distribution on its long axis and 0.2% imperfection of initial shape by the first buckling mode. From these curves, we can see that the nonlinear effect is clearly expressed at some critical nodes after the bifurcation phenomenon is come out in overall roof.

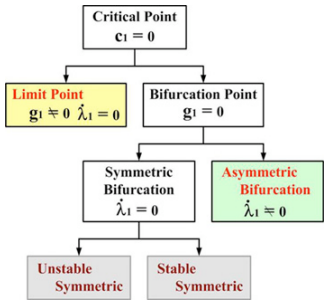


Figure 14: Critical points

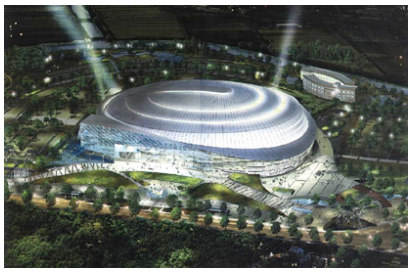

Figure 15: Speedom

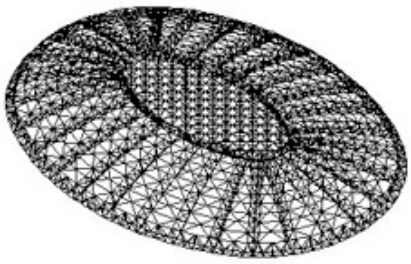

Figure 16: Discretized mesh

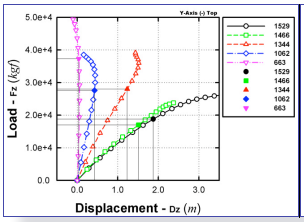


Figure 17: Top nodes(-)

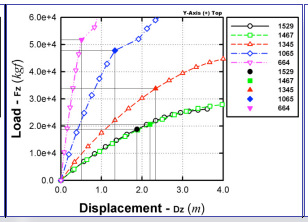


Figure 18: Top nodes(+)

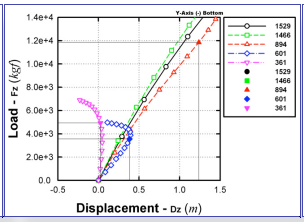


Figure 19: Bottom nodes(-)

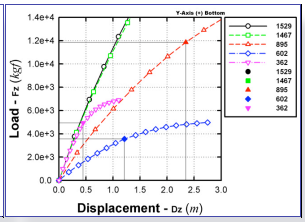


Figure 20: Bottom nodes(+)

## 5. Conclusions

In this study, author has introduced a new nonlinear analysis program NASS, short for Nonlinear Analysis for Spatial Structures. NASS, the first of its kind, is being developed for both soft and hard structures to get nonlinear solutions and to target a general purpose computational program.

Using some examples, NASS ability had been tested in both soft and hard structures, and we could see that the nonlinear program offers reliable results.

## References

[1] Kim SeungDeog et al., “Dynamic instability of shell-like shallow trusses considering damping,” Computer & Structures, Vol. 64, No. 1-4, 1997. 5., pp. 481-489.

[2] Kim SeungDeog et al., “A fuzzy optimum design of axisymmetrically loaded thin shells of revolution,” Structural Engineering and Mechanics, Vol. 7, No. 3, 1999. 3., pp. 277-288.

[3] Kim SeungDeog et al., “A study of nonlinear dynamic instability of hybrid cable dome structures,” Structural Engineering and Mechanics, Vol. 15, No. 6, 2003. 6., pp. 653-668.

Proceedings of the 6th International Conference on
Computation of Shell and Spatial Structures
IASS-IACM 2008: "Spanning Nano to Mega"
28-31 May 2008, Cornell University, Ithaca, NY, USA
John F. ABEL and J. Robert COOKE (eds.)

# Lateral buckling load formulation for multi-strut beam string structures

Jaeyeol KIM*, Minger WU

* Department of Architectural Engineering, Hyupsung University
Kyunggi-Do, 445-745, Korea
jjaerinim@empal.com

## Abstract

In the beam string structure (BSS), the moment in the beam is effectively reduced by means of the strings and the struts. As a result, the beam is very slender and the BSS is suitable to cross a long span. In the BSS, the struts can be considered as supports for the beam through the strings. Usually, the struts are in compression, they should be designed to avoid buckling, but few researches can be found about the lateral buckling of the struts in the BSS. Because one end of the struts is jointed to the beam while the other end is connected to the strings, the buckling of the struts not only depends on the length of the struts and the stiffness of the joints, but also depends on the rise and the lateral stiffness of the beam, the layout of the strings and the number of the struts. In this paper, the lateral buckling load of the struts in multi-strut beam string structure is formulated.

## 1. Introduction

Consider a one-strut beam string structure (BSS), the simplest BSS, as shown in Figure 1. The beam in the BSS is assumed to be an arch while the connection between the beam and the strut is a rigid joint. Because of the compression in the strut, which is caused by the tension in the strings, the strut should be designed carefully to avoid buckling [1].

The buckling of the strut may happens in in-plane's direction (the beam-strut plane), or in lateral direction (perpendicular to the beam-strut plane, see Figure 1). The two ends of the strut are constrained by the strings and the beam in the in-plane's direction, so the buckling in this direction can be calculated easily. On the other hand, the lateral buckling is influenced by the rise of the beam, the rotational stiffness of the joint and the lateral stiffness of the beam. The phenomenon of the lateral buckling of the struts in the BSS is very similar to the beam's lateral buckling. Numerous researches on the beam's lateral buckling and the bracing stiffness have been carried out. A summary of the research advances on this topic can be found in [2]. But no reference concerning the lateral buckling of the struts in the BSS can be found according to the author's surveys.

In order to reduce the maximum bending moment in the beam more effectively, more than one strut can be used in the BSS. In this paper, the lateral buckling load is formulated for the multi-strut BSS.

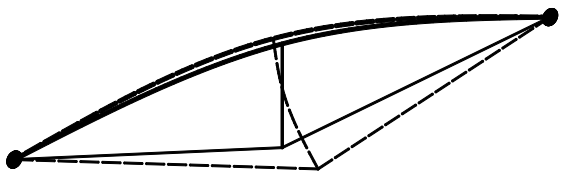

Figure 1: Lateral buckling of the strut in the BSS

## 2. Lateral buckling load formulation

To simplify the analysis, we assume that the layout of the deformed BSS under the load $w$ as shown in Figure 2 is symmetrical to the middle point of the span so only the half of the structure is analyzed. The struts are vertically set and the inclination caused by the load is ignored in formulating process. The rise $b_i$ of the beam is measured from the horizontal line as shown in Figure 2. The BSS has $2n$-1 ($n$≥1) struts and the joints between the struts and the beam are semi-rigid.

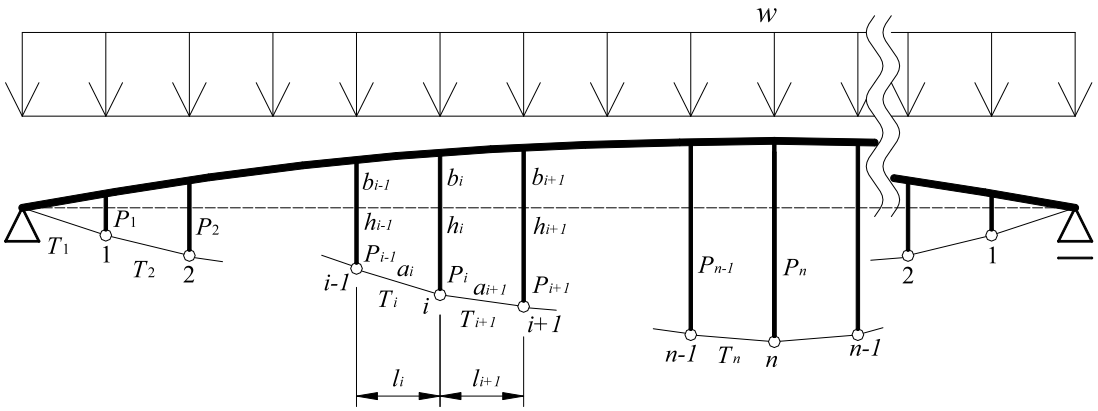


Figure 2: Multi-strut BSS

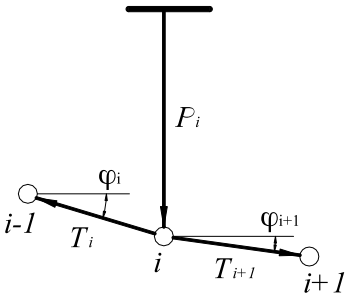


Figure 3: Equilibrium at node $i$

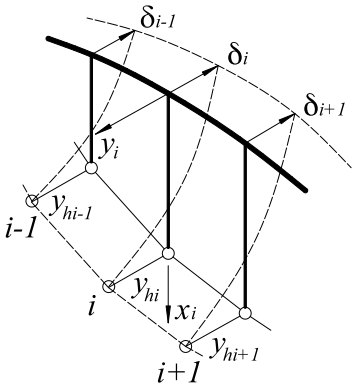


Figure 4: Lateral deformation of the struts and the beam

| | | | |
|---|---|---|---|
| $P_i$ | axial force of strut; | $T_i$ | tension of string; |
| $b_i$ | rise of the beam; | $l_i$ | distance between struts $i$ and $i$-1; |
| $h_i$ | length of strut; | $a_i$ | length of string, $a_i = \sqrt{l_i^2 + (h_i - b_i - h_{i-1} + b_{i-1})^2}$ . |

The lateral stiffness of the beam has a great influence on the buckling load of the strut. The low lateral stiffness of the beam may cause a very low buckling load. Here the lateral stiffness of the beam is considered in analysis while the torsion of the beam is neglected because the torsional stiffness can been considered in the joint rotational stiffness.

In order to simplify the analysis, we assume that the resultant force of the two strings' tensions at one node passes along the axis of the corresponding strut. From Figure 3, we have

$$T_i \cos\varphi_i - T_{i+1} \cos\varphi_{i+1} = 0 \quad T_i \sin\varphi_i - T_{i+1} \sin\varphi_{i+1} = P_i \tag{1}$$

where $\varphi_i$ and $\varphi_{i+1}$ are the angles of strings $i$ and $i$+1 (see Figure 3).

For the multi-strut BSS, it is obviously that the struts buckle to the same lateral direction if the lateral buckling of the struts occurs. Let the strut $i$ have a small lateral deformation $y_i$ as shown in Figure 4, at the same time, lateral deformation $\delta_i$ of the beam takes place. The lateral curvature of the strut $i$ can be expressed as

$$E_i I_i \ddot{y}_i = -\left[\frac{y_{hi} - y_{hi-1}}{a_i} T_i - \frac{y_{hi+1} - y_{hi}}{a_{i+1}} T_{i+1}\right](h_i - x_i) + P_i(y_{hi} - y_i) \tag{2}$$

where $x_i$ and $y_i$ are the two coordinate axes shown in Figure 4, $E_iI_i$ is the lateral bending stiffness of strut $i$, $y_{hi}$ is the lateral displacement at node $i$.

The boundary condition for Eq.(2) is written as

$$\begin{cases} y_i(0) = -\delta_i \\ \dot{y}_i(0) = M_{0i}/k_{\theta i} \\ y_i(h_i) = y_{hi} \end{cases} \tag{3}$$

In Eq.(3), $k_{\theta i}$ is the rotational stiffness of the semi-rigid joint between strut $i$ and the beam, $M_{0i}$ is the moment of the strut at $x_i$=0.

$$M_{0i} = -\left[\frac{y_{hi} - y_{hi-1}}{a_i} T_i - \frac{y_{hi+1} - y_{hi}}{a_{i+1}} T_{i+1}\right] h_i + P_i(y_{hi} + \delta_i) \tag{4}$$

The lateral deformation of the strut and the tension in strings cause the lateral force in the beam. If the beam is not laterally constrained completely, it becomes laterally deformed under the lateral force. The lateral deformation $\delta_i$ of the beam can be written as

$$\delta_i = \sum_{j=1}^{n} c_{ij} y_{hj} \tag{5}$$

$c_{ij}$ in Eq.(5) can be calculated from the lateral stiffness of the beam.

Let

$$\gamma_i = \lambda_i h_i \quad , \quad \lambda_i = \sqrt{\frac{P_i}{E_i I_i}} \quad , \quad e_i^1 = \frac{h_i}{l_i} \quad , \quad e_i^2 = \frac{h_i}{l_{i+1}} \quad , \quad \alpha_i = \frac{b_i}{h_i} \quad , \quad \beta_i = \frac{h_i k_{\theta i}}{E_i I_i} \tag{6}$$

by solving Eq.(2) and using boundary condition Eq.(3), we have

$$\begin{aligned} &\left[\left(\frac{\gamma_i}{\beta_i} + \frac{1}{\gamma_i}\right) e_i^1 \tan\gamma_i - e_i^1\right] \cdot y_{hi-1} + \\ &\left[\left(\tan\varphi_i - \tan\varphi_{i+1} - e_i^1 - e_i^2\right)\left(\frac{\gamma_i}{\beta_i}\tan\gamma_i - 1\right) - \frac{1}{\gamma_i}\left(e_i^1 + e_i^2\right)\tan\gamma_i\right] \cdot y_{hi} + \\ &\left[\left(\frac{\gamma_i}{\beta_i} + \frac{1}{\gamma_i}\right) e_i^2 \tan\gamma_i - e_i^2\right] \cdot y_{hi+1} + \\ &\left(\frac{\gamma_i}{\beta_i}\tan\gamma_i - 1\right)\left(\tan\varphi_i - \tan\varphi_{i+1}\right)\sum_{j=1}^{n} c_{ij} y_{hj} \\ &= 0 \end{aligned} \tag{7}$$

Writing Eq.(7) for all the struts, we obtain a matrix equation

$$(\mathbf{A} + \mathbf{B}) \cdot \mathbf{y_h} = \mathbf{0} \tag{8}$$

where matrix **A** is summarized from the first three items of the left side of Eq.(7) and matrix **B** from the fourth item. Matrix **B** indicates the influence of the lateral deformation of the beam. $\mathbf{y_h}$ is the vector of the lateral displacements of the struts. Through setting the determinant of the coefficient matrix of Eq.(8) be zero, the buckling condition is obtained.

$$\det(\mathbf{A}+\mathbf{B})=0 \tag{9}$$

## 3. Example of 3-strut BSS

An example for finding the lateral buckling load of 3-strut BSS is given to illustrate the method suggested in the paper.

By using Eq.(7), we get Eq.(10) for node 1 and Eq.(11) for node 2.

$$\begin{aligned}&\left[\left(\tan\varphi_1-\tan\varphi_2-e_1^1-e_1^2\right)\left(\frac{\gamma_1}{\beta_1}\tan\gamma_1-1\right)-\frac{1}{\gamma_1}\left(e_1^1+e_1^2\right)\tan\gamma_1+\left(\frac{\gamma_1}{\beta_1}\tan\gamma_1-1\right)\left(\tan\varphi_1-\tan\varphi_2\right)c_{11}\right]y_{h1}+\\&\left[\left(\frac{\gamma_1}{\beta_1}+\frac{1}{\gamma_1}\right)e_1^2\tan\gamma_1-e_1^2+\left(\frac{\gamma_1}{\beta_1}\tan\gamma_1-1\right)\left(\tan\varphi_1-\tan\varphi_2\right)c_{12}\right]y_{h2}=0\end{aligned} \tag{10}$$

$$\begin{aligned}&\left[\left(\frac{\gamma_2}{\beta_2}+\frac{1}{\gamma_2}\right)e_2^1\tan\gamma_2-e_2^1+\left(\frac{\gamma_2}{\beta_2}\tan\gamma_2-1\right)\tan\varphi_2 c_{21}\right]y_{h1}+\\&\left[\left(\tan\varphi_2-e_2^1\right)\left(\frac{\gamma_2}{\beta_2}\tan\gamma_2-1\right)-\frac{1}{\gamma_2}e_2^1\tan\gamma_2+\left(\frac{\gamma_2}{\beta_2}\tan\gamma_2-1\right)\tan\varphi_2 c_{22}\right]y_{h2}=0\end{aligned} \tag{11}$$

If the beam is laterally constrained and the rigid joints between the struts and the beam are used, we have $c_{11}=c_{12}=c_{21}=c_{22}=0$ and $\beta_1,\beta_2\to\infty$. In this case, by letting the determinant of the coefficient matrix of Eqs.(10,11) be zero, one equation for finding $\gamma_1$ and $\gamma_2$ is obtained.

$$\det\begin{bmatrix}\tan\varphi_2-\tan\varphi_1+\left(e_1^1+e_1^2\right)\left(1-\dfrac{\tan\gamma_1}{\gamma_1}\right) & -e_1^2\left(1-\dfrac{\tan\gamma_1}{\gamma_1}\right)\\ -e_2^1\left(1-\dfrac{\tan\gamma_2}{\gamma_2}\right) & -\tan\varphi_2+e_2^1\left(1-\dfrac{\tan\gamma_2}{\gamma_2}\right)\end{bmatrix}=0 \tag{12}$$

On the other hand, by using Eq.(1) for $P_1/P_2$ and Eq.(6), we have

$$\frac{\gamma_1}{\gamma_2}=\frac{h_1}{h_2}\sqrt{\frac{E_2I_2}{E_1I_1}\frac{\tan\varphi_1-\tan\varphi_2}{2\tan\varphi_2}} \tag{13}$$

Using $\gamma_1$ and $\gamma_2$ obtained from Eqs.(12, 13), the critical compression $P_{cr1}$ and $P_{cr2}$ in strut 1 and 2 when the lateral buckling happens are calculated.

## Acknowledgement

This research was supported by a grant (code C106A1030001-06A05300510) from Large Spatial Structures Program funded by Ministry of Construction & Transportation of Korea government.

## References

[1] Tomka P. Lateral stability of cable structures. International Journal of Space Structures 1997; 12(1): 19-30.

[2] Galambos TV. Guide to stability design criteria for metal structures, Fifth Edition. John Wiley & Sons; 1998.

Proceedings of the 6th International Conference on
Computation of Shell and Spatial Structures
IASS-IACM 2008: “Spanning Nano to Mega”
28-31 May 2008, Cornell University, Ithaca, NY, USA
John F. ABEL and J. Robert COOKE (eds.)

# A simple procedure for the analysis of hyperelastic 3D membrane structures

Vinicius ARCARO*

* College of Civil Engineering, UNICAMP, Brazil
Avenida Albert Einstein 951, Campinas, SP 13083-852, Brazil
vinicius@arcaro.org

## Abstract

This text presents a mathematical modeling of a triangular membrane finite element. The deformation gradient tensor is written in terms of nodal displacements for a simple triangular element. The invariants of the Right Cauchy-Green deformation tensor are written in terms of nodal displacements. The total potential energy is minimized using a quasi-Newton method. In case of a compressible material, the total potential energy is minimized with respect to the nodal displacements and element thicknesses. The idea of minimizing the total potential energy to find equilibrium was first introduced by Coyette and Guisset [1] for cable network analysis. The advantages of this approach are: It is not necessary to derive the stiffness matrix; it is not necessary to solve any system of equations; it allows a simple static analysis instead of a pseudo-dynamic analysis (dynamic relaxation with kinetic damping). The computer code uses the limited memory BFGS to handle large scale problems as described by Nocedal and Wright [4]. It also employs a line search procedure with safeguards as described by Gill and Murray [2] and Lasdon [3]. The source and executable computer codes are available for download from the author's website (http://www.arcaro.org/tension/).

## 1. Introduction

Figure 1 show the geometric entities used in the mathematical expressions.

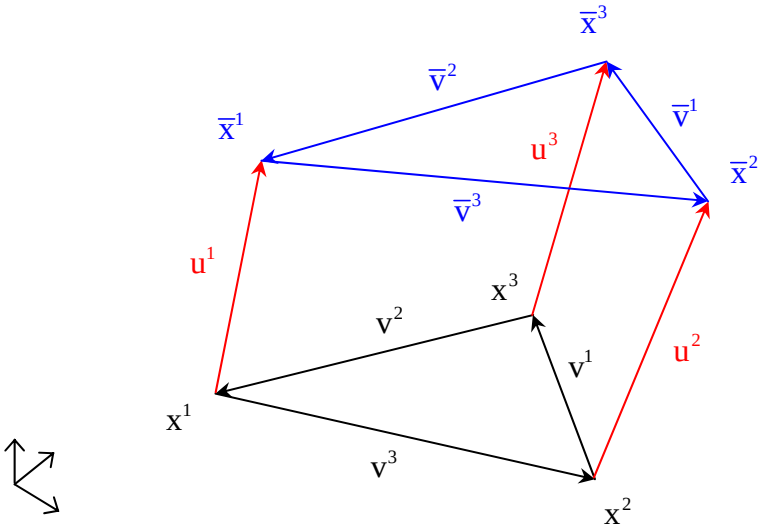


Figure 1

$$\bar{v}^1 = v^1 + u^3 - u^2 \tag{1}$$

$$\bar{v}^2 = v^2 + u^1 - u^3 \tag{2}$$

$$\bar{v}^3 = v^3 + u^2 - u^1 \tag{3}$$

$$w = \frac{v^1 \times v^2}{\left\| v^1 \times v^2 \right\|} \tag{4}$$

$$\alpha = w^T \left( v^1 \times v^2 \right) \tag{5}$$

$$\bar{w} = \frac{\bar{v}^1 \times \bar{v}^2}{\left\| \bar{v}^1 \times \bar{v}^2 \right\|} \tag{6}$$

$$\bar{\alpha} = \bar{w}^T \left( \bar{v}^1 \times \bar{v}^2 \right) \tag{7}$$

$$w^i = w \times v^i \ , \ i = 1,2,3 \tag{8}$$

$$\bar{z}^1 = \left[ \left( v^1 \right)^T v^1 \bar{v}^2 - \left( v^1 \right)^T v^2 \bar{v}^1 \right] \tag{9}$$

$$\bar{z}^2 = \left[ \left( v^2 \right)^T v^1 \bar{v}^2 - \left( v^2 \right)^T v^2 \bar{v}^1 \right] \tag{10}$$

The unit vectors w and $\bar{w}$ are orthogonal to the element's surface in the undeformed state and deformed state respectively. Notice that these vectors points toward the observer, when nodes associated with the element appear counterclockwise.

The scalars $\alpha$ and $\bar{\alpha}$ are equal to twice the area of the element in the undeformed state and deformed state respectively.

The scalars $\delta$ and $\bar{\delta}$ are equal to the thickness of the element in the undeformed state and deformed state respectively.

## 2. Deformation gradient tensor

The deformation gradient tensor can be written as:

$$F = I + \frac{1}{\alpha}\left[ u^1 \left( w^1 \right)^T + u^2 \left( w^2 \right)^T + u^3 \left( w^3 \right)^T \right] + \left( \frac{\bar{\delta}}{\delta} \bar{w} - w \right) w^T \tag{11}$$

Notice that,

$$Fv^1 = \bar{v}^1 \tag{12}$$

$$Fv^2 = \bar{v}^2 \tag{13}$$

$$Fv^3 = \bar{v}^3 \tag{14}$$

$$F\left( \delta w \right) = \left( \bar{\delta} \bar{w} \right) \tag{15}$$

## 3. Right Cauchy-Green deformation tensor

The invariants of the right Cauchy-Green deformation tensor and its derivatives with respect to displacements can be written as:

$$c_1 = \frac{1}{\alpha^2}\left[\left(\bar{v}^2\right)^T \bar{z}^1 - \left(\bar{v}^1\right)^T \bar{z}^2\right] + \left(\frac{\bar{\delta}}{\delta}\right)^2 \tag{16}$$

$$\frac{\partial c_1}{\partial u^1} = \frac{2}{\alpha^2}\bar{z}^1 \tag{17}$$

$$\frac{\partial c_1}{\partial u^2} = \frac{2}{\alpha^2}\bar{z}^2 \tag{18}$$

$$\frac{\partial c_1}{\partial \bar{\delta}} = \frac{2}{\delta}\left(\frac{\bar{\delta}}{\delta}\right) \tag{19}$$

$$\begin{aligned} c_2 = & \\ & + \frac{1}{\alpha^4}\left[\left(\bar{v}^1\right)^T \bar{v}^1 \left(\bar{z}^2\right)^T \bar{z}^2 - \left(\bar{v}^1\right)^T \bar{v}^2 \left(\bar{z}^2\right)^T \bar{z}^1\right] + \\ & + \frac{1}{\alpha^4}\left[\left(\bar{v}^2\right)^T \bar{v}^2 \left(\bar{z}^1\right)^T \bar{z}^1 - \left(\bar{v}^1\right)^T \bar{v}^2 \left(\bar{z}^2\right)^T \bar{z}^1\right] + \\ & + \left(\frac{\bar{\delta}}{\delta}\right)^4 \end{aligned} \tag{20}$$

$$\frac{\partial c_2}{\partial u^1} = \frac{4}{\alpha^4}\left(\bar{v}^2\right)^T \bar{z}^1 \bar{z}^1 - \frac{4}{\alpha^4}\left(\bar{v}^1\right)^T \bar{z}^1 \bar{z}^2 \tag{21}$$

$$\frac{\partial c_2}{\partial u^2} = \frac{4}{\alpha^4}\left(\bar{v}^2\right)^T \bar{z}^2 \bar{z}^1 - \frac{4}{\alpha^4}\left(\bar{v}^1\right)^T \bar{z}^2 \bar{z}^2 \tag{22}$$

$$\frac{\partial c_2}{\partial \bar{\delta}} = \frac{4}{\delta}\left(\frac{\bar{\delta}}{\delta}\right)^3 \tag{23}$$

$$c_3 = \left(\frac{\bar{\delta}\bar{\alpha}}{\delta\alpha}\right)^2 \tag{24}$$

$$\frac{\partial c_3}{\partial u^1} = \frac{2\bar{\alpha}}{\alpha^2}\left(\frac{\bar{\delta}}{\delta}\right)^2 \left(\bar{w} \times \bar{v}^1\right) \tag{25}$$

$$\frac{\partial c_3}{\partial u^2} = \frac{2\bar{\alpha}}{\alpha^2}\left(\frac{\bar{\delta}}{\delta}\right)^2 \left(\bar{w} \times \bar{v}^2\right) \tag{26}$$

$$\frac{\partial c_3}{\partial \bar{\delta}} = \frac{2\bar{\alpha}^2}{\delta\alpha^2}\left(\frac{\bar{\delta}}{\delta}\right) \tag{27}$$

## 4. Solution strategy

### 4.1 Incompressibility

Set invariant 3 of the deformation gradient tensor F equal to 1 and solve for the deformed thickness. Simplify the expressions for the invariants of the right Cauchy-Green deformation tensor C. In this way, the thickness of the element in the deformed state is not a variable anymore. Minimize the total potential energy with respect to the displacements.

$$\frac{\bar{\delta}\bar{\alpha}}{\delta\alpha} = 1 \Rightarrow \bar{\delta} = \frac{\delta\alpha}{\bar{\alpha}} \tag{28}$$

### 4.2 Compressibility

In an attempt to improve convergence and also to avoid a solution with negative thickness, the repetition of the following steps, using the initial thickness and zero displacements as starting point, can be used to minimize the total potential energy.

- Fix all thicknesses. Minimize the total potential energy with respect to the displacements only.
- Fix all displacements. Minimize the total potential energy with respect to the thicknesses only.
- Minimize the total potential energy with respect to the displacements and thicknesses.
- Replace any negative thickness by the initial thickness.

## 5. Examples

A Quasi-Newton method (limited memory self scaling BFGS) with implementation as described by Nocedal and Wright [4] and cubic interpolation line search with safeguards as described by Gill and Murray [2] and Lasdon [3] was used to minimize the total potential energy. Computer codes and examples for incompressibility and compressibility can be downloaded from the author's website (http://www.arcaro.org/tension/).

## 6. Conclusion

The analysis is static analysis instead of a pseudo-dynamic analysis. It is not necessary to derive the stiffness matrix expressions. It is not necessary to solve system of equations. It can handle large scale problems. It does not matter if the structure is under constrained. The approach can be extended for line and tetrahedral elements.

## References

[1] Coyette JP and Guisset P. Cable network analysis by a nonlinear programming technique. *Engineering Structures* 1988; **10**: 41-46.

[2] Gill PE and Murray W. Newton type methods for unconstrained and linearly constrained optimization. *Mathematical Programming* 1974; **7**:311-350.

[3] Lasdon L. Optimization theory for large systems. Prentice Hall, 1970.

[4] Nocedal J and Wright SJ. Numerical Optimization. Springer-Verlag, 1999.

Proceedings of the 6th International Conference on
Computation of Shell and Spatial Structures
IASS-IACM 2008: “Spanning Nano to Mega”
28-31 May 2008, Cornell University, Ithaca, NY, USA
John F. ABEL and J. Robert COOKE (eds.)

# Test on mechanical properties of architectural membrane

Kang-geun PARK *, Seong-kee YOON*, Woo-hong JEON**

*Professor, Architectural Engineering Dept., Pusan National Univ.
**Reseacher, Korea Apparel testing & Research Institute(Pusan)
Cheonghakri, Samrangrangjineup, Miryang, Gyeongnam, 627-706, Korea
sampgk@pusan.ac.kr

## Abstract

The purpose of testing method study for membrane material in large span structures is provided the basic testing method about the testing standard are assorting and surveying for applying the construction and calculation of structures. Some problems of membrane materials have fire proofing, lack of strength, self cleaning, tear capacity, durability, heat insulation, sound insulation and elasticity. For the solution of this problems, it will be tested the mechanical properties of architectural membrane material. In this study, the development on test method of membrane material will be proposed and tested by tensile strength, tearing resistance, cycling test, etc. The testing information of basic membrane gives the method of rational design, and can provide the safety truth and validity of large span building in spatial structure. And it will be analyzed to the shape finding and stress concentration of architectural membrane. The development of new material opened up new possibility for membrane structures by the testing results of membrane material.

## 1. Introduction

In modern times, synthetic fibres and grass fibres have been created, and coating materials that improve durability and fireproofing and waterproofing qualities have been newly developed. As a result, membrane structures have become as durable and safe structural material. Membrane structures are characterized by translucency, lightness of weight and application are suited its frame for large spaces. The development of new membrane materials open up new possibility for membrane structures. Comparable to stainless steel in its durability, it came to be recognized as a permanent structural material. It has proven truly epochal for development of membrane structures. Permanent buildings using this material, especially large arenas, began to be widely constructed in the 1970s. At first, it was feared that a glass fibre fabric was not sufficiently durable and would disintegrate in time. However, this membrane material, which is hardened with fluor polymers, has already maintained sufficient strength for 24 years. However there are problems of durability and the soiling if its surface. A design method based a allowable unit stress is generally used for membrane structures, and 4.0 is frequently adopted throughout the world as the safety for a membrane material. The purpose of testing method study for membrane and cable material in large span structures is provided the basic data about the testing standard are assorting and surveying for applying the construction and calculation of structures. Membrane materials are characterized by translucency, lightness of weight and earlier membrane materials were foldable, but PTFE coated glass fibre fabric membrane is not folded or detached. It is permanent building material

and is incombustible, strong, durable and self-cleaning. It is important that advantage be taken of the merits of membrane when membrane structures used in combination with other structures. Some problems of membrane materials have fire proofing, lack of strength, self cleaning, tear capacity, durability, heat insulation, sound insulation and elasticity. Cable has some problems of connection part in construction of structures. For the solution of these problems, it has to test the membrane and cable material. Achieved the researches successfully, it is expected that advanced technical power and improved testing method for spatial structure material. This value is by no means satisfactory, but it takes into account the possible deterioration in the strength of the membrane material. In view of the low cost of membrane material, this safety factor may be the lowest society will accept. Past example of accidents in membrane structures show that damage is caused by tears spreading in the membrane material. Tears are generated by localized incidents that are not accounts for in structural calculations. The safety of membrane structures therefore depends a great deal on the design of details. In this study, the development on test method of membrane material was studied to the test of tensile strength, tearing resistance, and cycling load test, etc.

## 2. Testing Method of Membrane

### 2.1 Tensile strength test

Tensile test is applied a force longitudinally to a test piece of a specified length and width at a constant rate of extension and obtained determination of values for breaking strength and elongation from the recorded force-elongation curve. Unless otherwise specified, cut five test pieces in the machine direction and five in the cross-machine direction, ensuring that they are all taken at least 100㎜ from edge and are equally distributed across the width and length of the specimen. Cut the test pieces 20-50㎜±0.5㎜ wide and of sufficient length to allow a jaw separation of 100㎜ more, thus avoiding risks due to local heterogeneity of nonwovens or to undue cutting of long-fiber nonwovens. Wider test pieces and different forms of clamping may be used by agreement between the interested part, a note of these special conditions should be included in the test report. This method specified in ISO 5081(Textile-Woven-Determination of breaking strength and elongation).

### 2.2 Biaxial tensile test

Using the tensile test method in which forces can be simultaneously applied in both warp and weft directions of a specimen of membrane material, load with a certain load ratio is applied in warp and weft directions to obtain the load strain relationship, then tensile stiffness and Poission's ratio are calculated from the load strain relationship. The width of relevant part of the specimen and length of the arm are 16 cm or more, and the specimen should have a symmetrical shape with respect to its warp and weft directions. Slit should be cut along the arms at intervals of 3-5. The specimen corners should be rounded with a radius of 5-15 cm. Final results are expressed as the means of more three specimens. Load ratio test have to 1:1, 2:1, 1:2, 1:0, 0:1 and the standard tensile rate is generally 2-4 mm/min. This method specified in The Standard of Testing Method for Membrane Material(The membrane Structures Association of Japan, 1995).

### 2.3 Tearing resistance test

Tearing resistance test is marking of a trapezoid on a test piece and clamping of the non-parallel sides of the trapezoid in the jaws of a tensile testing machine, and application of a continuously increasing extension to the test piece in such a way that a tear propagates across

its width. Unless otherwise specified, cut five test pieces in the machine direction and five in the cross-machine direction. The edge of the specimen should not normally form part of the test piece (75±1)㎜×(150±2)㎜. Mark each test piece with an isosceles trapezoid using the template. Other dimensions, respecting the general proportions of the original test piece, may be agreed between interested part, especially in order to reproduce some in-use conditions cannot be compared. Condition the test pieces as specified in ISO 193. Carry out the testing in the standard atmosphere for testing. At the start of the test, set the clamps 25±1㎜ apart and operate the machine at 100㎜/min. If the test piece does not tear at the cut, no result shall be registered. The tearing force will not usually be a single value but will generally appear as a series of maxima and minima.

### 2.4 Fatigue resistance

To estimate the fatigue resistance of the membrane material, as fatigue stress of rain and wind which the membrane material used in membrane structures would be exposed, sinusoidal tensile stress can be applied to the base material and joints of the membrane material. After the cycle repeated $5 \times 10^3$ times and $3 \times 10^5$ times, the tensile strength and elongation at break are measured, and the change in strength is determined. Even after $5 \times 10^3$ times and $3 \times 10^5$ times of the fatigue test, the base material and joints have the retention of tensile strength of about 90%. The material is proved to have sufficient endurance. The clamped parts have to be reinforced by thermally welding the same material.

### 2.5 Folding endurance

When the material is used as an architectural membrane material, it is expected that the material will be folded during processing and construction. Therefore, to confirm the folding endurance of the material, tensile test is conducted after folding test is performed. It is to be confirmed that the material do not decrease in tensile strength when it was folded along a 3-mm-diam bar. When the material is used as an architectural membrane material, it is expected that workers may trample on the folded parts of the material during processing and construction. To confirm the endurance of the folded parts to repeated application of pressure, tensile test is conducted after the material is folded by a cylinder type folding tester. After the material was folded by pressing with a weight of about 1 kg/cm, the strength can reduce to about 80%. It is proved that the material did not show so significant deterioration in tensile strength. However, since the material uses glass fiber for its base, it is necessary to fold it with utmost care. After a 5.1-kg roll is rolled on a folded part of the membrane material 10 times, the tensile strength is measured to determine the decrease in strength.

### 2.6 Creep properties

Creep test was conducted to confirm the creeping state of the material under axial tensile load. In the creep test under the predetermined conditions, the base material and joints of the membrane material don't show any abnormalities. Dimensions of test piece are to be 30㎜ wide and 320㎜ long. Number of test piece has to be specimens in warp direction and in weft direction. Gap between two gage marks is to be 100㎜and clamp distance is 200㎜

### 2.7 Elastic constant

Tension was applied to the membrane material in the warp and weft directions to determine the tensile rigidity based on the relationship between stress and strain. The test was conducted in accordance with testing method standard. Testing equipment has to use plane biaxial tensile

tester machine. Load ratio test have to 1:1, 2:1, 1:2, 1:0, 0:1, and loading pattern is conducted in accordance with testing method standard.

### 2.8 Shear rigidity

The shear rigidity values necessary for design and analysis of membrane structures were determined. The test is conducted in accordance with Testing Method Standard MSAJ/M01-1993 (established by Membrane Structures Association of Japan). In a square frame, of which each corner can be freely rotated, a specimen with the prescribed tension introduced in the directions of warp and weft is mounted with the frame aligned in the direction of woven thread. Under this condition, the square frame is deformed in the diagonal direction, and in-plane shear stiffness is determined from the relationship between the load obtained and displacement. The square frame of the tester has a pin t each corner and inner dimensions of 16cm x 16cm or more. From the load displacement curve, the first load displacement is removed. From the average curve between the 2$^{nd}$ and 3$^{rd}$ load displacement points are connected.

## 3. Testing Result of Membrane Material

### 3.1 Mechanical capacity test of glass fiber membrane

This part is shown the experimental results on tensile strength, cycling load test and tearing strength of membrane material for using spatial structures. Testing specimen is PTFE coated glass fiber and the thickness is 0.58mm. In the results of tensile strength, the elastic modulus of glass fiber coating membrane was obtained 3618-4443 N/㎟. The break strain of glass fiber membrane was given to 5.83-7.08%.. In the results of tearing strength, PTFE coated glass fiber is showed the weakness of tearing resistance capacity.

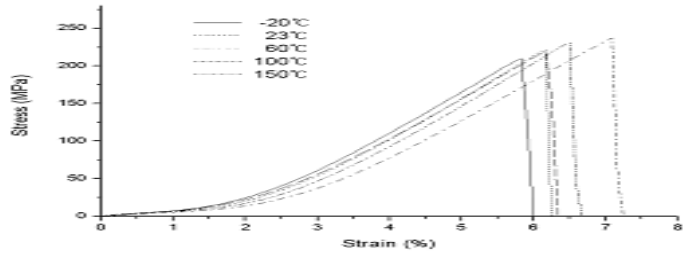


Fig.1 Stress-strain curve of glass fiber membrane by temperature

(Specimen size: width 25mm x clamp space 100mm)

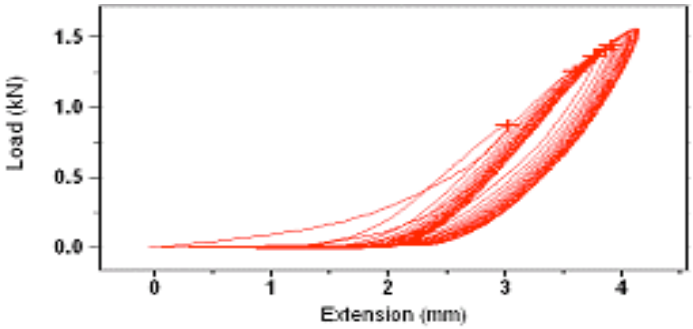


Fig.2 Cycling load test of glass fiber membrane

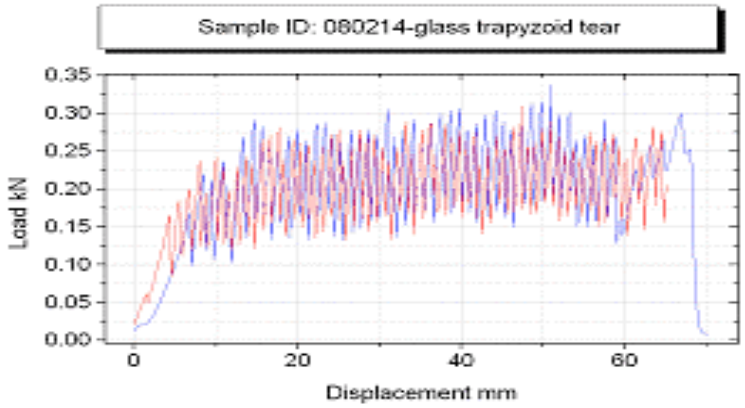


Fig.3 Tearing strength test of glass fiber membrane

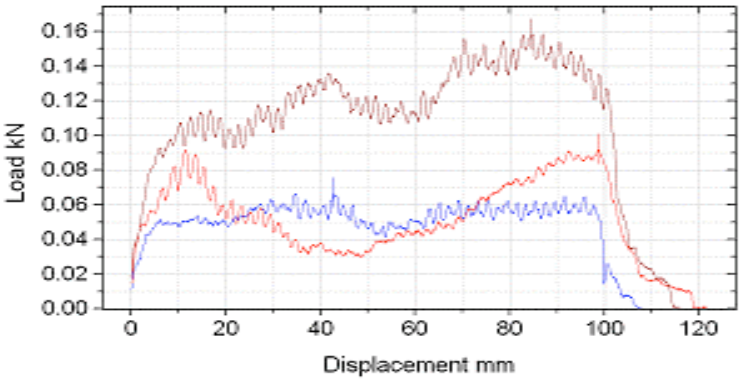


Fig.4 Welding contact capacity test of glass fiber membrane

### 3.2 Mechanical capacity test of polyester membrane

Testing specimen is PVDF coated polyester of thickness 1.05mm. In the results of tensile strength, PVDF coated polyester membrane showed the weakness of initial tensile resistance capacity. The elastic modulus of polyester coating membrane was obtained 375-389 N/㎟. The break strain of polyester membrane was given to 24-29%. This paper proposed the testing methods and experimental results of tearing resistance strength of membrane material for using spatial structures.

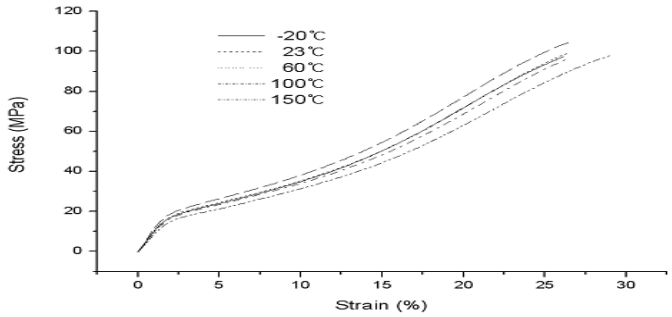

Fig.5 Stress-strain curve of polyester membrane by temperature
(Specimen size: width 25mm x clamp space 100mm)

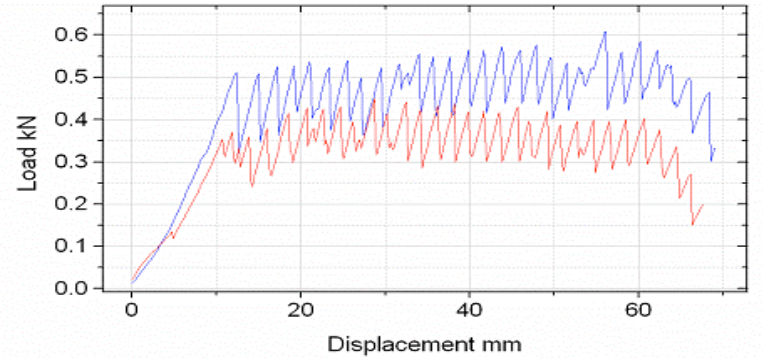


Fig.6 Tearing strength test of polyester membrane by temperature

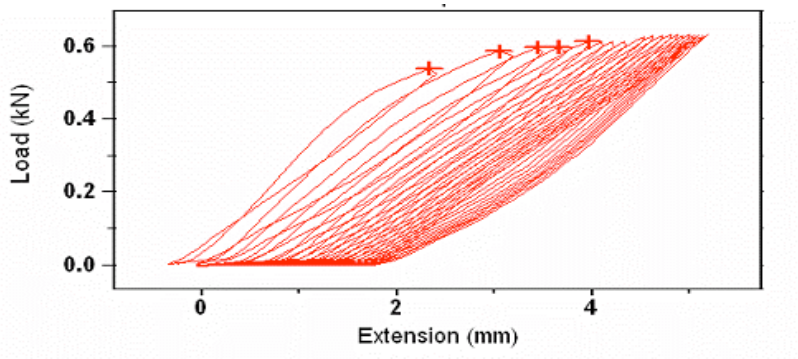


Fig.7 Cycling load test of polyester membrane

### 3.3 Mechanical capacity test of ETFE film

ETFE is abbreviation of Ethylene Tetra Fluoro Ethylene, a sort of colorless and transparent granules. ETFE film has superior ability of daylight transmission and elongation. The tensile strength of ETFE film changes from 40Mpa to 60Mpa and the tensile at break can get to about 300-400%.

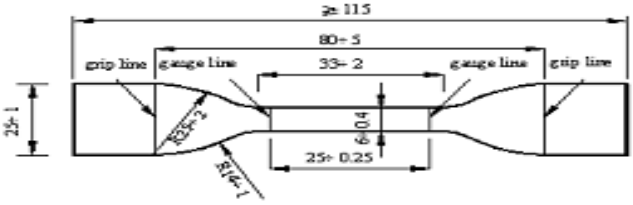


Fig.8 Dumbbell-shaped specimen of ETFE film(t=0.25mm)

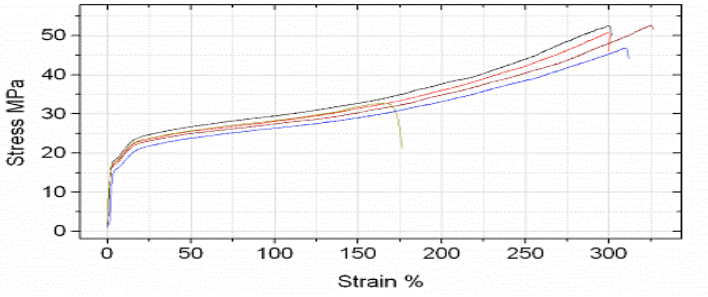


Fig.9 Stress-strain curves of ETFE film(t=0.25mm)

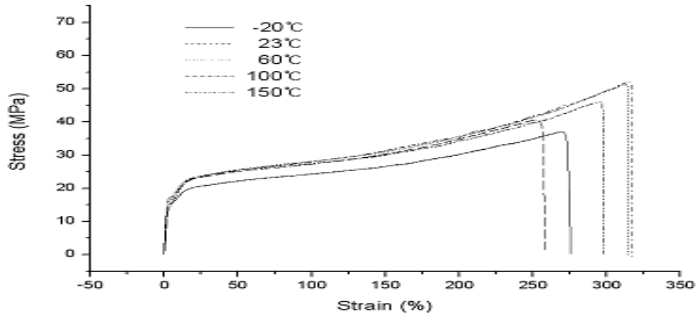


Fig.10 Stress-strain curves of ETFE film by temperature

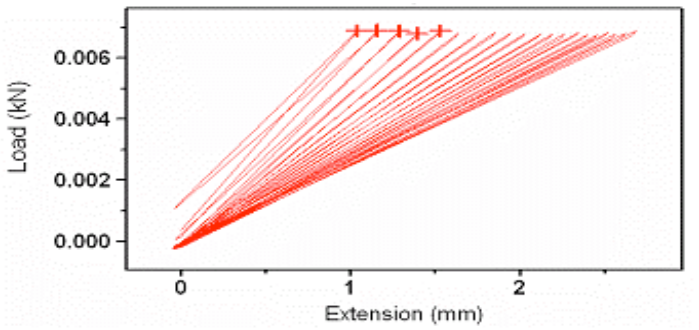


Fig.11 Cycling load test of ETFE film

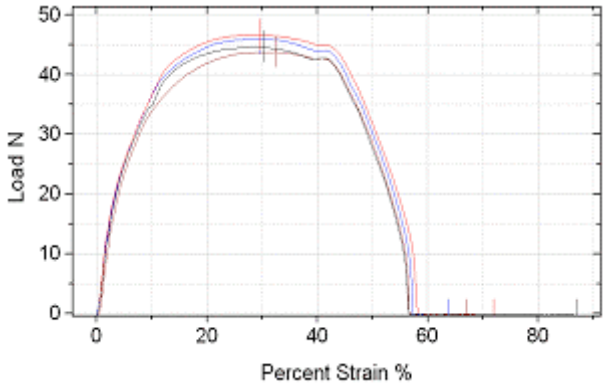

Fig.12 Tearing strength test of ETFE film

## 4. Conclusion

This paper was proposed the mechanical testing method of membrane material, and some testing results was showed about tensile test, tearing resistance test and cycling load test. The testing information of basic membrane material gives the method of rational design, and can provide the safety truth and validity of large span building in spatial structure. The development of new material opened up new possibility for membrane structures by the testing results of membrane material.

## Acknowledgement

This research was supported by a grant (Code #'06-R&D B03) from Cutting-edge Urban Development Program funded by Ministry of Construction & Transportation of Korean government.

## References

[1] Membrane Designs and Structures, Modern Architecture Series of GA, 1999

[2] Technical Information on Permanent Architectural membrane Material, Research & Development Division of Chukoh Chemical Industries, Feb. 2005

[3] The Standard of Testing Method for Membrane Material, The membrane Structures Association of Japan, 1995

[4] H. MINANI, "A Multi-Linear Approximation on the Nonlinear Extension Curves of PTFE-Coated Glass Fiber Fabric and the Application", *Journal of Structural and construction Engineering of Architectural Institute of Japan* , No.436, June, 1992

[5] Y. HINO, K. ISHII, "An Evaluation Method on the Material Nonlinearity in the Analysis of Membrane Structures", *Research Report on Membrane Structures of the Membrane Structure Association of Japan,* 1994

Proceedings of the 6th International Conference on
Computation of Shell and Spatial Structures
IASS-IACM 2008: "Spanning Nano to Mega"
28-31 May 2008, Cornell University, Ithaca, NY, USA
John F. ABEL and J. Robert COOKE (eds.)

# Simplified computer-aided formfinding procedures applied to light weight structures

Juan Gerardo OLIVA SALINAS*, Eric VALDEZ OLMEDO

* Professor, Dr.-Ing., Arq.
Universidad Nacional Autonoma de México
School of Architecture - Edificio Unidad de Posgrado, P. B.
Ciudad Universitaria, Mexico, D. F., CP 04510 - Mexico
jgos@servidor.unam.mx

## Abstract

In this paper we will show simplified geometric programs developed to determine the form of specific cases of grid-shells, as well as of tent constructions. The development of these computer programs is based on the appropriate knowledge and application of analytical geometry, whereas some special algorithms based on the simplified electronic modeling of membranes applying the computer programs Auto-Cad and Excel, will be explained and discussed. Some examples of grid-shells and newly built tent constructions designed and developed by applying the procedures described before, will show the efficiency and accuracy of the simplified computer programs and algorithms specially developed for these purposes.

## 1. Introduction

Computers offer powerful tools to design and analyze light weight structures. In the field of architectonical design, nowadays it is possible to apply the virtual reality to practically any form conceived and designed by the architect or structural designer. Nevertheless, the building of physical models is still very useful for the active architects, as well as for the students; but just to obtain enough parameters to evaluate the approximately final shapes of the structure. The precise formfinding procedures of light weight structures in order to determine their geometry or the cutting patterns of specific cases, like tent constructions or grid-shells, can be very quickly carried out by using computers and the many computer programs developed by special groups worldwide. Unfortunately, many of these computer programs are very expensive and the students or most of the active architects are unable to acquire this software.

## 2. Description

First, we will briefly describe the computer program GEOG (**Geo**metry of **G**rid-Shells). With GEOG we can generate a translation surface where the generatrix and directrix are catenaries. In previous papers and Simposia, we have reported the many advantages that this special shapes offer: the shape corresponds to a funicular system (the inverted form of a hanging net); four symmetrical nodes are on the same plane (plane plates of glass, timber or reinforced concrete for instance, can be used as covering elements); a universal knot-bars system with constant length allows the building of grid-shells with different curvatures using always the same structural elements. Wit GEOG we can generate different shape possibilities in a few seconds and afterwards we can decide the final geometry to be built whose geometrical definition is completely delivered. During a sabbatical staying at the University of Essen in Germany, we joined the geometry delivered by GEOG with the computer programs developed by the research groups of Professor G. Thierauf, thus it was possible to start immediately after the final shape was defined with the mechanical calculations and structural behavior of the structure. The figure 1 shows a grid-shell calculated with GEOG, an example of calculations with Professor Thierauf's program and a grid-shell for a Court House conceived, designed and built in Mexico City.

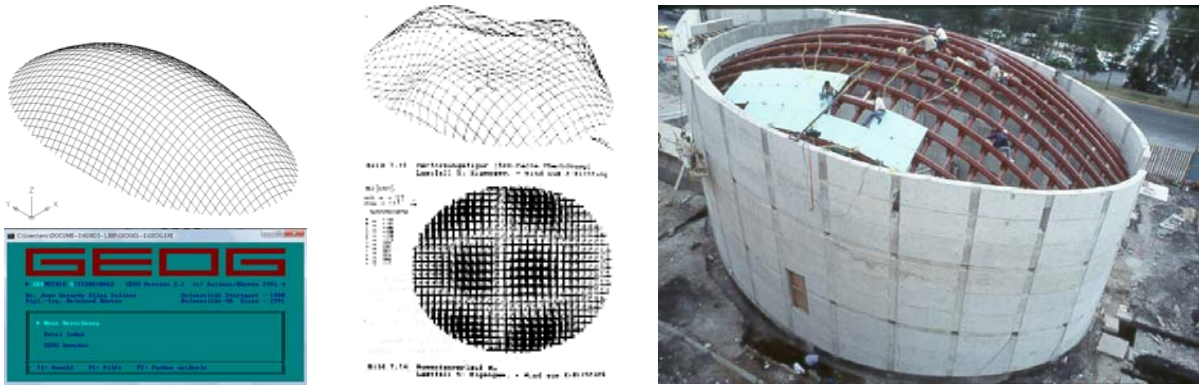


Figure 1: Example of computational formfinding process for a grid-shell

We will now describe computer aided processes that we have developed in our Laboratory of Structures and that we have called *electronic modeling*. These processes are analog to common physical modeling methods, like modeling clay for instance; but in this case assisted by computers and the Auto-CAD and Excel programs. Instead of modeling physical material, we model virtual nets modifying their geometry and looking for obtaining a proper and right geometry. A correct geometry is the basis for an equilibrated mechanical behavior, in accordance with the building materials and the final shape of the structural project.

The electronic modeling process will be described with the formfinding methods applied to the project of a tension structure for a historical building in the downtown of Mexico City. Figs. 2 and 3. The challenge was to cover two courtyards with different dimensions in order to cover a surface of approximately 540 m2.

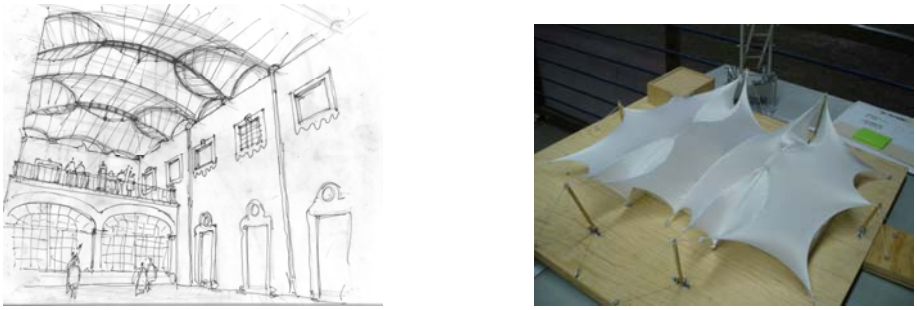

Figure 2: First sketches and physical study model of a tension structure

First, let us consider a section of the surface related to a fix three-coordinate system; its boundary lines and its anchoring points, secondly let us fill these surfaces with straight lines with 45° on the xy-plane and finally let us generate on this surface, a new net with parallel lines to the x- and y-axis and with variable curvature. This will be the first digital net, which will be used to start the electronic modeling of the surface:

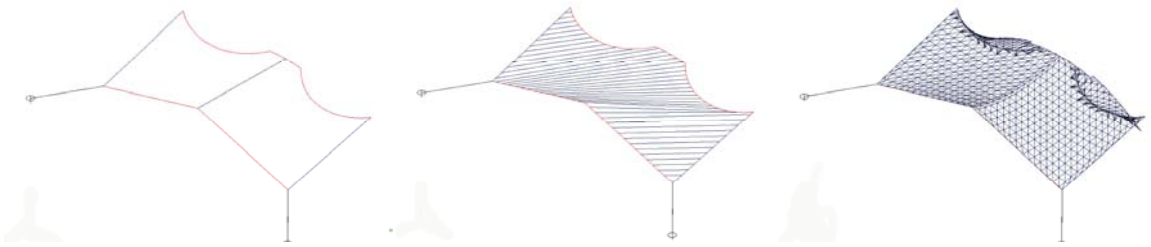

Figure 3: Three stages of the electronic modeling of a tension structure

It follows an interactive analysis process for each knot, which will be moved in the z-axis in such a way that a homogeneous anticlastic curvature is guaranteed on every single point of the surface. This surface can be manipulated in order to be adapted to the desired shape conceived by the architect or structural designer or in order to enhance its capability to drain the raining waters for instance. Once the final net is accepted by architects and structural engineers, the determination of the cutting patterns is determined. In the next figures we can compare the final surfaces obtained through our electronic modeling with the surfaces generated with the program EASY developed at the University of Berlin, Germany.

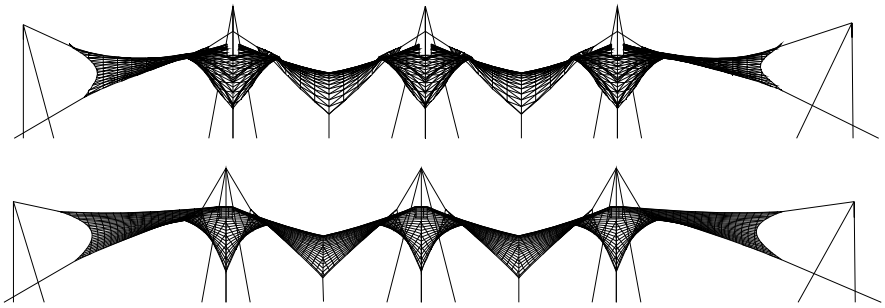

Figure 3: Compare the upper membrane generated by electronic modeling with the lower membrane generated with EASY

Finally, let us discuss another way of electronic modeling and formfinding process for the project developed by a group of Mexican architects at the University of Mexico for the roof of the Aquarium of the Mexican Centre of the Turtle. The project is inspired in the shell of the Lute Turtle (Dermochelys coriacea). The covered area is 2,400 m2 and it is located in Mazunte, Oaxaca.

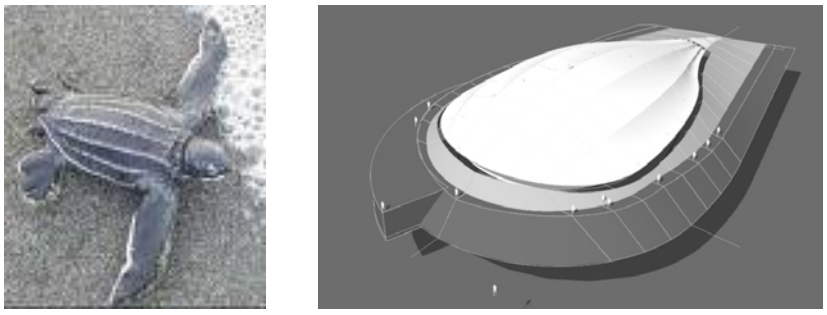

Figure 4: Lute Turtle *(Dermochelys coriacea)* and architectural proposal

The architects determined the final external form they wanted, but they did not know how to solve a structural system adequate to their conception. Thus they asked us for developing a proposal based on a structural system of timber and metal and a double sheet of tensile membrane necessary because of thermic isolation. It was an interesting challenge for us and after a few days of analysis of possible proposals; finally we got out that a suitable solution would be a combination of a synclastic curvature surface (a translation surface) with a HP-Surface (Hyperbolic paraboloid Surface.) Parabolas were used for the directrix and generatrix curves of both translation surfaces.

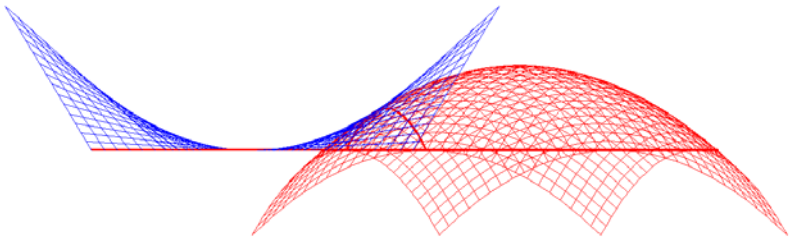

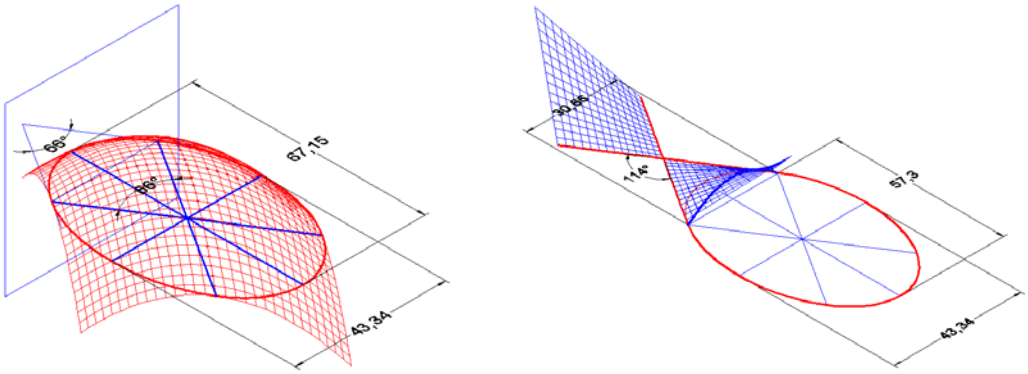


Figure 5: Combination of a synclastic with an anticlastic surface.

The obtained combination of the synclastic with the anticlastic surfaces produces a continuous clean surface and fulfilled the formal intentions of the architects.

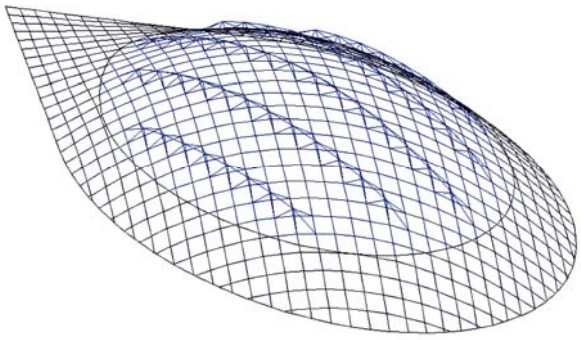

Figure 5: Final project

## 3. Conclusions

The examples, formfinding methods and computational calculations shown in this paper enable us to assert that by applying geometry with simplified computational methods, it is possible to develop formfinding processes to conceive, design and build light weight structures. Examples of grid-shells and tension structures, as well as a combination of both structural systems developed in our Laboratory of Structures will be shown. Our research works show an inexpensive alternative proposal for students, architects and structural designers. We are conscious of the limitations of these proposals and it is not our aim to compete with the research groups all over the world, who have developed very efficient and suitable computer programs for the design, calculation and construction of light weight structures.

## Acknowledgement

The attendance to this Conference is sponsored by the program *PAPIIT* of the *Direccion General de Asuntos del Personal Academico, UNAM.*

## References

[1] Oliva Salinas JG, Ontiveros Hernandez MJ, Valdez Olmedo E, Zetina Gargollo C, Structural geometry applied to the design and construction of shell and spatial structures. *Proceedings of the International Symposium IASS-APCS Beijing, China* 2006; 482.

[2] http://ciepfa.posgrado.unam.mx/laboratoriodeestructuras/

Proceedings of the 6th International Conference on
Computation of Shell and Spatial Structures
IASS-IACM 2008: "Spanning Nano to Mega"
28-31 May 2008, Cornell University, Ithaca, NY, USA
John F. ABEL and J. Robert COOKE (eds.)

# Shape formation of ETFE film cushion by heat and pressure considering visco-plastic characteristics

Masaya KAWABATA*, Kaoru NISHIKAWA

Associate Professor, Department of Architecture and Building Science, Yokohama National University
79-5 Tokiwadai, Hodogaya, Yokohama, Japan
mkwbt@ynu.ac.jp

## Abstract

As the start for establishing the 3 dimensional extension technique, this paper discusses the visco-elastic characteristic and its evaluation method of ETFE film, and considers the example and effect of the curved surface fabrication by extension. Since yield strength per unit width serves as an extremum, 10 to 20% of extension is the optimal. It was checked that smooth curved surface form has been formed with target rise near 10% as a result of 3 dimensional extension, and that the stable rigidity had been acquired.

## 1. Introduction

There are advantages in ETFE film , such as that it is transparent, lightweight, easy to manufacture a large-sized panel by heat-sealing both films and excelling in the durability over ultraviolet rays. Therefore, it is well used in membrane structure construction in recent years. Film is low strength compared with textile materials, and since thermal expansion and a viscous distortion are large, it is used as the short air cushion of the distance between fulcrums in many cases. In the manufacture field of plastics, high strengthening by drawing of a film is general. it is possible to fabricate a low rise panel of high yield strength or to fabricate a high rise panel of smooth curved surface with little weld line. As the start for establishing the 3 dimensional extension technique, this paper discusses the visco-elastic characteristic and its evaluation method of ETFE film, and considers the example and effect of the curved surface fabrication by extension.

## 2. Drawing of ETFE film

SS curve of an ETFE film is shown in Figure 1. Usually, as for film structure, it is common to design with allowable stress design method or ultimate strength design method. By allowable stress design, the stress corresponding to the 2% strain of near the 1st yield point is often made into the upper limit stress. By ultimate strength design, the stress corresponding to the 10% strain of near the 2nd yield point is often made into the upper limit stress. In the manufacture field of plastics, high strengthening by drawing of a film is general, and fabrication of PET resin products and films are the example of representation. Figure 2 shows the relation between a strength ratio (A) and the rate of extension, the relation between the thickness ratio at the time of biaxial extension (B), and the rate of extension, and the relation between the product (C) of (A) and (B), and the rate of extension about the ETFE film. The yield stress ratio is the value, which divided the each stress of SS curve by the 1st yield point stress. In calculation of the thickness after biaxial extension, the extension ratio is assumed to be 1:1 and volume is assumed to be constant. From a viewpoint of raising yield strength, the extension effect of the range of the extension rate of 300 to 400% is high. However, drawing is accompanied by reduction in thickness, the fall of tear resistance, impact resistance fall, and the fall of wear and abrasion resistance. Therefore, it is not appropriate to use a film with the high degree of extension for the outer layer of air cushions. Taking the above characteristics into consideration, since yield strength per unit width (C) serves as an extremum, 10 to 20% of extension is the optimal.

Consideration of anisotropy is indispensable necessity although it is easy at the time of material manufacture to extend the direction of 1 axis like the roll direction. It seems that there is no example performed positively

since the rise becomes high although it is possible at the time of the inflation of a film cushion to perform biaxial extension by pressure. Extension by prestretching is possible also at the time of panel attachment. As for especially a simple-shaped panel, it is possible for the plane film which does not perform draping to also carry out curved surface fabrication by prestretching and high-pressure extension. If the above-mentioned method is used, it is possible to fabricate a low rise panel of high yield strength or to fabricate a high rise panel of smooth curved surface with little weld line. It seems that however, there is also no example which performed these positively. The first reason is because there is a possibility of producing partial plastic elongation at the time of prestretching, since the strain of the 1st yield point of ETFE film is only 2%. The second reason is that the structural analysis technique as which SS curve in 2 to 20% of strain domain indicates a complicated visco-plastic behavior, and estimates this with sufficient accuracy is not yet established. So, as the start for establishing the above-mentioned technique, this paper discusses the visco-elastic characteristic and its evaluation method of ETFE film, and considers the example and effect of the curved surface fabrication by extension.

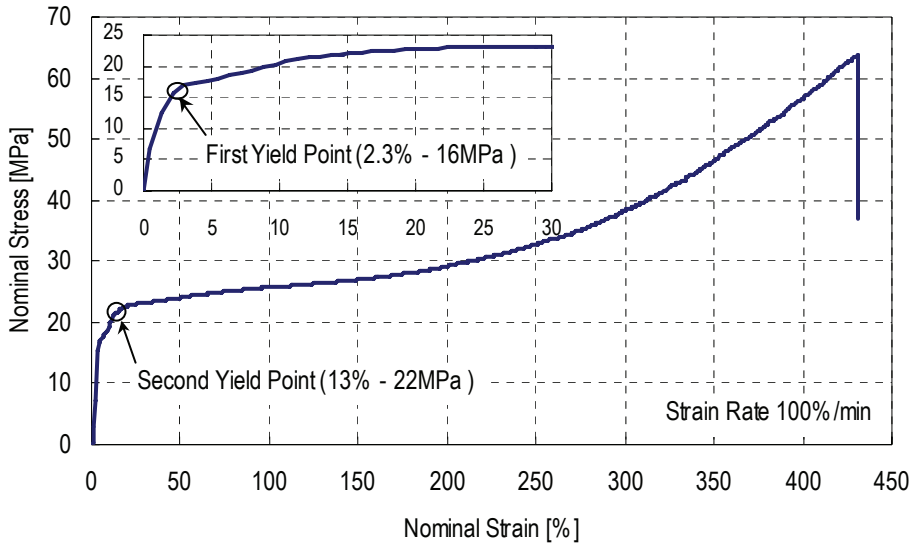


Figure 1: Stress strain curve of ETFE film

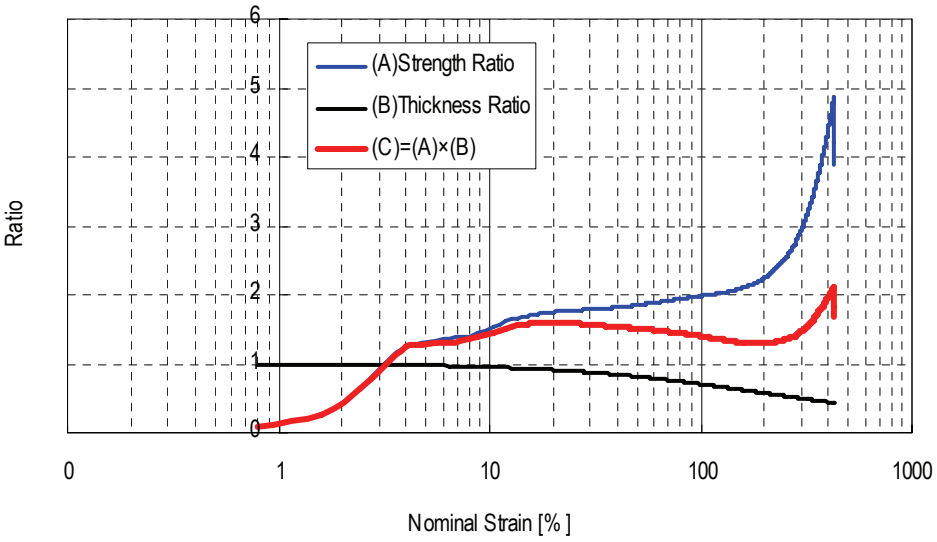


Figure 2: Drawing of ETFE film

## 3. Heating pressurization fabrication

The outline of a heating pressurization fabrication experiment is shown in Figure 3.

Procedure 1: Film panel (a plane, two sheets) is attached to a frame.

Procedure 2: Keeping at 60 ℃ within a heat insulation container, the inside of a cushion is pressurized (1st Inflation) and plastic deformation is added.

Procedure 3: At the room temperature of 20 ℃, the cushion is pressurized (2nd Inflation) to check shape and rigid stability.

Figure 4 shows the rise change and SS curve among inflation processes. Stress and strain of SS curve have calculated by having assumed an equally tensioned spherical surface. It was checked that smooth curved surface form has been formed with target rise near 10% as a result of 3 dimensional extension, and that the stable rigidity had been acquired. SS curve and the 1st yield points are shown in Figure 5 according to temperature. The strain of the 1st yield points are around 2%, and is almost the same at every temperature. On the other hand, the yield stress in 60 ℃ is almost half of the yield stress in 20 ℃, and temperature dependency of yield stress is strong. Figure 6 shows creep curves according to temperature. The creep strain of the ETFE film of normal temperature shows clearly that it becomes a nonlinear relation to load stress. If load stress becomes 50% or more of the 1st yield point especially, creep distortion will increase notably. The creep strain in 60℃ shows the tendency similar to the strain at the time of applying high load stress in normal temperature, and, as for this, it is considered to be a reason that the 1st yield point fell by the rise in heat. As mentioned above, under high temperature, since it is accompanied by the fall of yield stress, it becomes easy to perform plastic processing by low-pressure power. However, it needs to be cautious of that it is in the tendency for the viscous behavior of an ETFE film to advance very slowly, and creep strain being in an increase process, even if 72 hours pass. Therefore, it is important to evaluate a plasticity permanent strain and a viscosity time dependence strain by pressurization or extension by prestretching with sufficient accuracy.

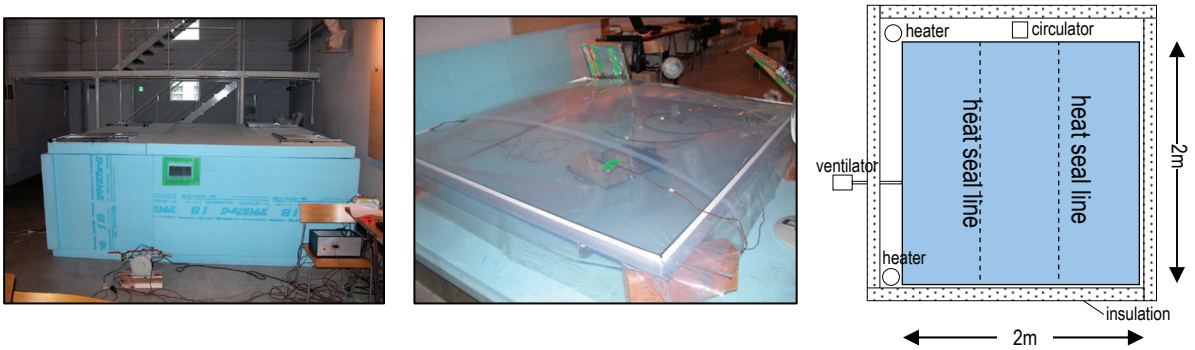


Figure 3: Heating pressurization fabrication experiment

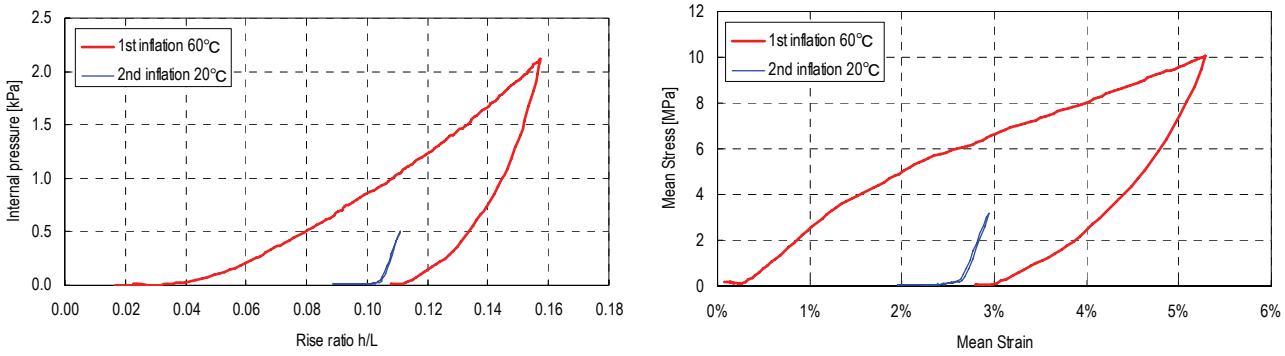


Figure 4: Rise change and SS curve during heating pressurization fabrication experiment

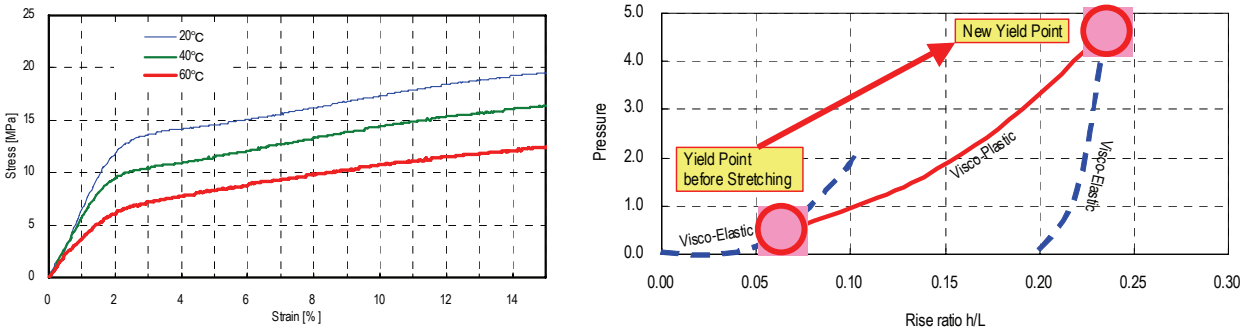


Figure 5: SS curves at different temperature

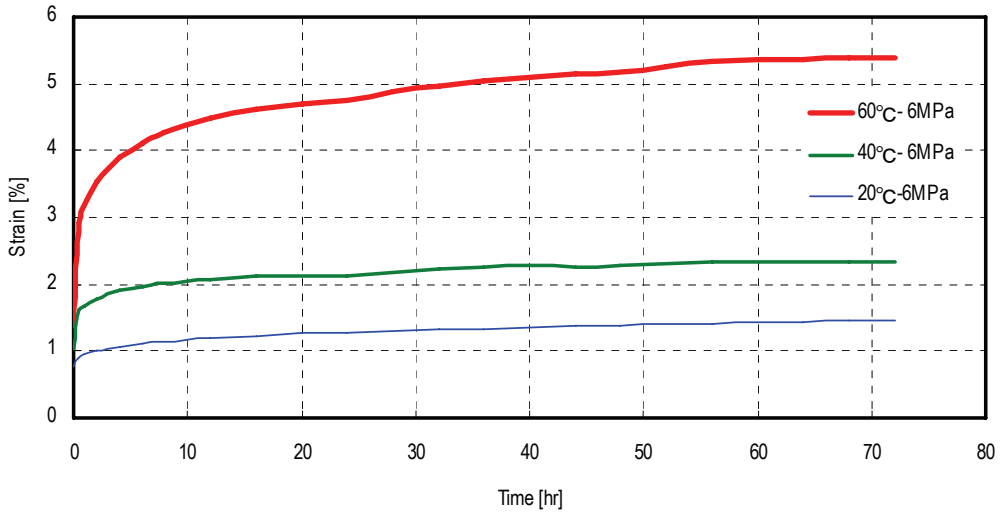


Figure 6: Creep curve at different temperature

## 4. Conclusion

Since yield strength per unit width serves as an extremum, 10 to 20% of extension is the optimal. It was checked that smooth curved surface form has been formed with target rise near 10% as a result of 3 dimensional extension, and that the stable rigidity had been acquired.

## References

[1] Schwitter C., "The Use of ETFE Foils in Lightweight Roof Constructions", Proc. of IASS Symposium 1994(Atlanta), pp622-631, 1994

[2] Kawabata M, Moriyama F. and Aida H., "Viscoelastic characteristic of ETFE film", vol 19, pp.1-8, Research Report on Membrane Structures 2005 (Japanese)

[3] Kawabata M. and Moriyama F.; "Study on Viscoelastic Characteristics and Structural Response of Film Membrane Structures", Proceedings of the IASS-APCS 2006 International Symposium, MB01.150~MB01.151, 2006

[4] Kawabata M.; " Viscoplastic Properties of ETFE Film and Structural Behavior of Film Cushion", Proceedings of the IASS 200 International Symposium, 2007

Proceedings of the 6th International Conference on
Computation of Shell and Spatial Structures
IASS-IACM 2008: "Spanning Nano to Mega"
28-31 May 2008, Cornell University, Ithaca, NY, USA
John F. ABEL and J. Robert COOKE (eds.)

# Shape finding of membrane structures by the natural force density method

Ruy M.O. PAULETTI*, Paulo M. PIMENTA

*Polytechnic School, University of São Paulo
P.O. Box 61548, 05424-970 São Paulo, Brazil
pauletti@usp.br

## Abstract

This work presents an extension of the force density method for the initial shape finding of cable and membrane structures, which leads to the solution of a system of linear equations. This method is called ***the natural force density method*** (see Pauletti and Pimenta [12]), and preserves the linearity of the original force density method. Furthermore, if it is applied iteratively in the lines prescribed herein, it may lead to a viable equilibrium configuration with a uniform, isotropic plane Cauchy stress state. This means that a minimal surface for a membrane can be achieved through a succession of viable configurations. This is an advantage, if compared to Newton's Method, which may also converge to a minimal solution, but through a series of unfeasible configurations.

## 1. Introduction

Since Frei Otto's pioneering works in the 1950's, taut structures (encompassing both cable and membrane structures) constitute an important research field in architecture and engineering. They are light, elegant and effective structures, whose applications range from large stadium roofs and high-rise building walls to pneumatic furniture or aerospace equipment. The design of taut structures is integrated to their analysis, in a process that includes procedures for shape finding patterning and load analysis. Some references on the design of taut structures are Haber and Abel [1], Knudson [2], Tabarrok and Qin [3], Moncrief and Topping [4] and Barnes [5].

A versatile way to pose the overall design process of taut structures is via the Finite Element Method (FEM). It directly provides, besides a viable shape, also a map of the stresses to which the structure is subjected. It is also adequate to determine the behavior of the structure under design loads, as well as to transfer data to the patterning routines. On the other hand, procedures based on the FEM or in other forms of structural analysis result in nonlinear analyses, and require specification of a convenient initial geometry, load steps and boundary conditions, which are not always defined ab initio.

An alternative method for finding viable configurations, which avoids the problems related to nonlinear analysis, is given by the force density method, which was first proposed in the context of cable nets (Schek [6], Linkwitz [7], Gründig *et al.* [8]). Some analogous procedures for the shape finding of membrane structures have already been proposed in the literature, e.g. Singer [9] and Maurin and Motro [10]. However, these procedures are not linear and thus require iterations for solution. In this way, the advantage of the original force density method is lost, and there is no clear reason to replace a nonlinear structural analysis by another nonlinear procedure.

With the aid of the natural approach introduced by Argyris [11] for the Finite Element Method, this work presents an extension of the force density method for the initial shape finding of cable and membrane structures, which leads to the solution of a system of linear equations. This method is called the natural force density method (see Pauletti and Pimenta [12]), and preserves the linearity of the original force density method. Furthermore, if it is applied iteratively in the lines prescribed herein, it may lead to a viable configuration with a

uniform, isotropic plane Cauchy stress state. This means that a minimal surface for a membrane can be achieved through a succession of viable configurations. This is an advantage, if compared to Newton's Method, which may also converge to a minimal solution, but through a series of unfeasible configurations.

## 2. Formulation

Consider a three-noded plane triangular finite element. Let $\ell_\alpha^r$ and $\ell_\alpha$, $\alpha = 1,2,3$, be the element side lengths at a reference and at a viable, equilibrium configuration, respectively. It can be shown that the equilibrium of this element can be expressed by three pair of loads acting along the sides of the element. We collect this loads into a ***natural force vector*** $\mathbf{P}_n = \begin{bmatrix} P_{n1} & P_{n2} & P_{n3} \end{bmatrix}^T$, and define the ***vector of the natural force densities*** according to $\mathbf{n} = \mathbf{P}_n = \begin{bmatrix} n_1 & n_2 & n_3 \end{bmatrix}^T = \mathbf{\Lambda}^{-1}\mathbf{P}_n$, where $\mathbf{\Lambda} = \text{diag}\begin{Bmatrix} \ell_1 & \ell_2 & \ell_3 \end{Bmatrix}$.

Thereafter, we show that, for prescribed natural force densities $\mathbf{n}$, there is a linear relationship between the natural force vector $\mathbf{P}_n$ and element nodal coordinates $\boldsymbol{\xi} = \begin{bmatrix} \boldsymbol{x}_1 & \boldsymbol{x}_2 & \boldsymbol{x}_3 \end{bmatrix}^T$, according to $\mathbf{P} = \mathbf{k}\boldsymbol{\xi}$, where $\boldsymbol{x}_I$, $I = 1,2,3$, are the position vectors of the element nodes at the equilibrium configuration and $\mathbf{k}$ is a constant *element stiffness matrix* given by

$$\mathbf{k} = \begin{bmatrix} (n_2 + n_3)\boldsymbol{I} & -n_3\boldsymbol{I} & -n_2\boldsymbol{I} \\ \cdot & (n_1 + n_3)\boldsymbol{I} & -n_1\boldsymbol{I} \\ sym. & \cdot & (n_1 + n_2)\boldsymbol{I} \end{bmatrix}. \tag{1}$$

We thus arrive to linear problem at the structural level, after assembling the load and stiffness contributions of all elements.

Instead of prescribing directly the natural force densities $\mathbf{n}$ for each element, it is more convenient to prescribe their 2nd Piola-Kirchhoff stresses $\boldsymbol{\sigma}$, which relate to their natural force densities according to $\mathbf{n} = V^r\mathbf{\Lambda}^{r-2}\boldsymbol{\mathcal{A}}^{r-1}\boldsymbol{\mathcal{C}}^r\boldsymbol{\sigma}$, where $V^r$ is the element volume at the reference configuration, $\mathbf{\Lambda}^r = \text{diag}\begin{Bmatrix} \ell_1^r & \ell_2^r & \ell_3^r \end{Bmatrix}$, and

$$\boldsymbol{\mathcal{C}}^r = \begin{bmatrix} (c_{11}{}^r)^2 & (c_{12}{}^r)^2 & \sqrt{2}c_{11}{}^r c_{12}{}^r \\ (c_{21}{}^r)^2 & (c_{22}{}^r)^2 & \sqrt{2}c_{21}{}^r c_{22}{}^r \\ (c_{31}{}^r)^2 & (c_{32}{}^r)^2 & \sqrt{2}c_{31}{}^r c_{32}{}^r \end{bmatrix}, \quad \boldsymbol{\mathcal{A}}^r = \boldsymbol{\mathcal{C}}^r\boldsymbol{\mathcal{C}}^{rT} = \begin{bmatrix} 1 & (c_3{}^r)^2 & (c_2{}^r)^2 \\ \cdot & 1 & (c_1{}^r)^2 \\ sym. & \cdot & 1 \end{bmatrix},$$

where $c_\alpha{}^r = -\left(\ell_\beta^r \ell_\gamma^r\right)^{-1} \boldsymbol{l}_\beta^r \cdot \boldsymbol{l}_\gamma^r$ are the cosines of the internal angles of the triangular finite element at the reference configuration (indexes $(\alpha, \beta, \gamma)$ cyclically permute).

## 3. Applications

As an application of the linear natural force density method, we consider the transformation of the same plane, square reference mesh into different surfaces, all of then determined in a single step. First row of Figure 1 shows two hypars generated by prescribing displacements on the four vertices, along with a uniform 2nd Piola-Kirchhoff stress field on the membrane and different normal loads at the border cables. Second row of Figure 1 shows the same reference square mesh transformed into two other shapes, simply prescribing displacements to some selected nodes.

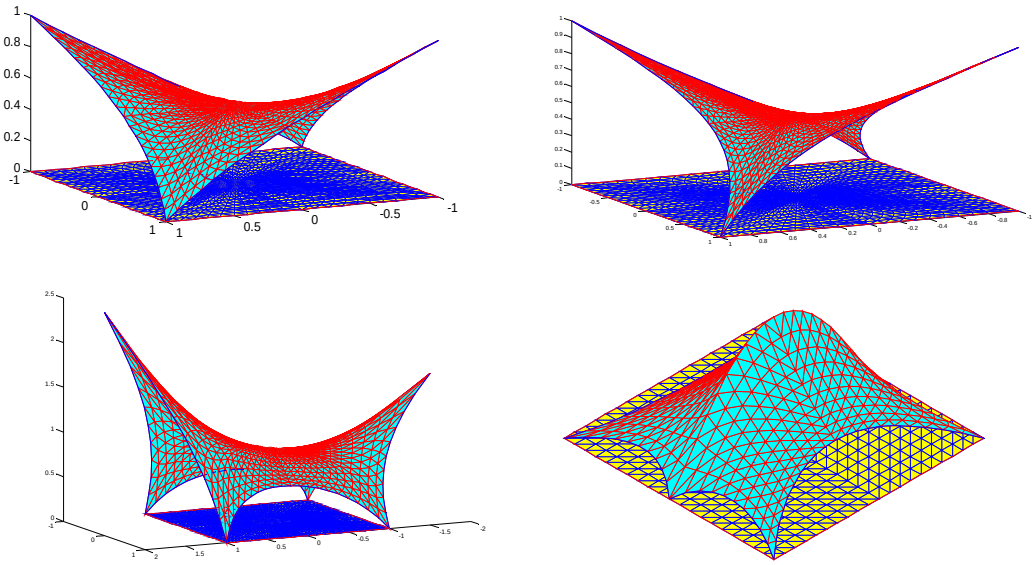

Figure 1 : Viable configurations generated through the imposition of different sets of nodal displacements and border cable force densities to the same plane squared reference mesh.

As a second example, we consider a helicoidal soap film surface, inspired by a physical experiment illustrated by Isenber [13]. A flat, unit square, reference geometry (Figure 2d) is deformed, such that sides S1 and S2 are transformed into small radial segments, of length 0.01. Side S2 is also displaced of 4.0, transversally to the reference plane. Side S3 is deformed into a helix. Side S4 is constrained to slip over the vertical axis, whose total length is 4.0. Figure 2a shows both the initial reference mesh and the resulting viable geometry, associated to a Cauchy stress field with quite high concentrations close to borders S2, S3 and S4. Subsequent iterations do not introduce significant alterations on geometry, but do smooth the stress field. After 10 iterations, a practically uniform and isotropic Cauchy stress field is achieved. Thus, the minimal surface associated with the prescribed boundary is indeed obtained.

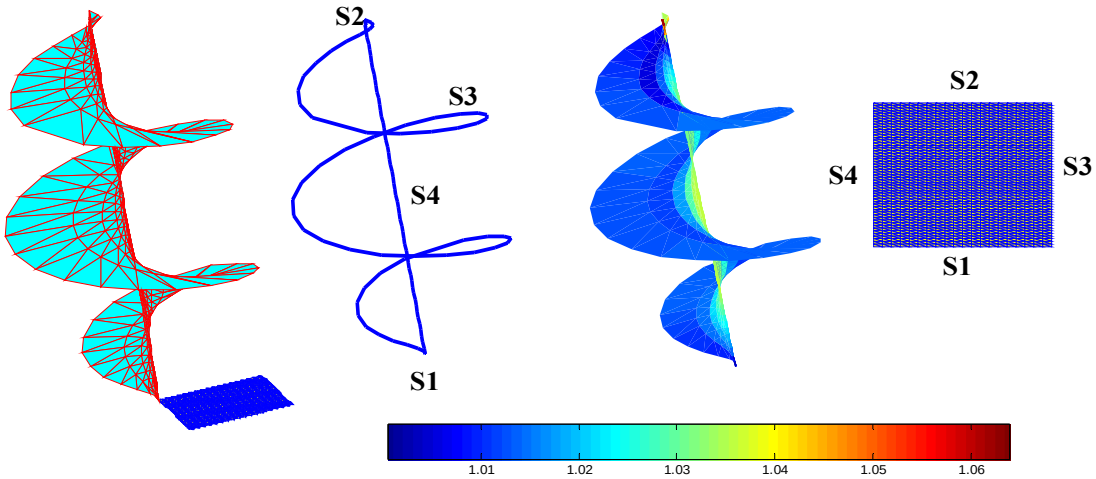


Figure – An helicoidal soap film

## References

[1] R.B. Haber, J.F. Abel, Initial equilibrium solution methods for cable reinforced membranes. Part I – Formulations, Comput. Methods Appl. Mech. Engrg. **30** (1982) 263–284, Part II – Implementation, Comput. Methods Appl. Mech. Engrg. **30** (1982) 285–306

[2] W.C. Knudson, Recent advances in the field of long span tension structures, Eng. Struct. **13** (1991) 164–177

[3] B. Tabarrok, Z. Qin, Nonlinear Analysis of tension structures, Comput. Struct. **45** (5/6) (1992) 973–984

[4] E. Moncrief, B.H.V. Topping, Computer methods for the generation of membrane cutting patterns, Comput. Struct. **37** (4) (1993) 441–450

[5] M.R. Barnes, Form and stress engineering of tension structures, Struct. Eng. Rev. 6 (3/4) (1994) 175–202

[6] H.-J. Schek, The force density method for form finding and computation of general networks, Comput. Methods Appl. Mech. Engrg. **3** (1974) 115–134

[7] K. Linkwitz, About form finding of double-curved structures, Eng. Struct. **21** (1999) 709–718

[8] L. Gründig, E. Moncrieff, P. Singer, D. Ströbel, A history of the principal developments and applications of the force density method in Germany 1970–1999, in: Proc. IASS-IACM 2000 – 4th International Colloquium on Computation of Shell & Spatial Structures (Shania, Crete, 2000)

[9] P. Singer, Die Berechnung von Minimalflächen, Seifenblasen, Membrane und Pneus aus geodätischer Sicht, PhD Thesis, University of Stuttgart, Institut für Anwendungen der Geodäsie im Bauwesen, 1995.

[10] B. Maurin, R. Motro, The surface stress density method as a form-finding tool for tensile membrane, Eng. Struct. **20** (1999) 712–719

[11] J.H. Argyris, P.C. Dunne, T. Angelopoulos, B. Bichat, Large natural strains and some special difficulties due to non-linearity and incompressibility in finite elements, Comput. Methods Appl. Mech. Engrg. **4** (2) (1974) 219–278

[12] R.M.O. Pauletti & P.M. Pimenta, The natural force density method for the shape finding of taut structures, submitted to Comput. Methods Appl. Mech. Engrg., 2007

[13] C. Isenberg. *The science of soap films and soap bubbles*, Dover Pub. Inc., New York, 1992.

Proceedings of the 6th International Conference on
Computation of Shell and Spatial Structures
IASS-IACM 2008: "Spanning Nano to Mega"
28-31 May 2008, Cornell University, Ithaca, NY, USA
John F. ABEL and J. Robert COOKE (eds.)

# Topology and shape of tensegrity structures

Jingyao ZHANG*, Makoto OHSAKI

*Dept. of Architecture & Architectural Engineering, Kyoto University
Kyoto University, Kyoto-Daigaku Katsura, Nishikyo, Kyoto 615-8540, Japan.
is.zhang@archi.kyoto-u.ac.jp

## Abstract

This study presents a random strategy for topology generation to investigate diversity of tensegrity structures. The process of finding shape in self-equilibrium with generated topology is separated into two design processes: (a) find the feasible force densities satisfying the non-degeneracy condition by the adaptive force density method proposed by the authors, and (b) determine nodal coordinates satisfying equilibrium equations by optimization techniques. A number of new stable structures, of which no struts physically interact with each other, are derived and presented as numerical examples.

## 1. Introduction

Tensegrity structures are prestressed pin-jointed structures, featured by their 'discontinuous' struts (in compression) balanced by 'continuous' cables (in tension) [1]. The main tasks in the design problem of tensegrity structures are to determine topology (connectivity of nodes and members) and stable shape (in terms of nodal coordinates) in self-equilibrium, hence it is also called *form-finding* problem. However, the topology issue has been discussed in only few studies, for example reference [2], while most of them concentrate on finding the self-equilibrium shapes with a given topology. Thus, the first objective in the study is to present a random strategy to investigate new topology for tensegrity structures.

Moreover, even for the same topology, there exist numerous different shapes satisfying equilibrium equations; not all of them are stable in three-dimensional space, though. The adaptive force density method [3] is such a numerical method that converges fast, and more importantly, guarantees a stable structure. Hence, it is adopted in the study to find the self-equilibrium shape for the topology generated by the proposed random strategy.

In summary, to study diversity of tensegrity structures, we adopt an iterative procedure with the following three processes in each step:

- Topology: Starting from a ground structure with every pair of nodes connected by a member, either cable or strut, one cable is removed randomly in each iterative step.
- Feasible force densities: Implement the adaptive force density method (AFDM) to find the feasible force densities that satisfy the non-degeneracy condition for a three-dimensional tensegrity structure.
- Self-equilibrium shape: Optimization techniques are utilized to find the optimal configuration subject to specified constraints, with the assumption that we do not have *a priori* knowledge about its final configuration.

## 2. Equilibrium and stability

Consider a tensegrity structure with $m$ members and $n$ nodes. Its topology is described by the connectivity matrix $\mathbf{C} \in \mathbb{R}^{m \times n}$: for member $k$ connected by nodes $i$ and $j$ ($i<j$), the $i$th and $j$th elements in the $k$th row of $\mathbf{C}$ are 1 and −1, respectively, while the other entries in the row are zero.

Let **x**, **y** and **z** ($\in \mathbb{R}^n$) denote nodal coordinates, and $\mathbf{q} = [q_1, \ldots, q_i, \ldots q_m]^{\mathrm{T}} \in \mathbb{R}^m$ denote force densities (prestress-to-length ratio). Hence, the coordinate differences in each direction can be calculated as **u = Cx, v = Cy, w = Cz**, and the geometry matrix **G**($\in \mathbb{R}^{m \times 6}$) is defined as

$$\mathbf{G} = [\mathbf{Uu}, \mathbf{Vv}, \mathbf{Ww}, \mathbf{Uv}, \mathbf{Uw}, \mathbf{Vw}], \tag{1}$$

where **U**, **V** and **W** are the diagonal forms of **u**, **v** and **w**, respectively.

Defining the force density matrix $\mathbf{E} \in \mathbb{R}^{n \times n}$ as

$$\mathbf{E} = \mathbf{C}^{\mathrm{T}} \mathrm{diag}(\mathbf{q}) \mathbf{C}, \tag{2}$$

self-equilibrium equations of the structure in each direction can be written as

$$\mathbf{Ex} = \mathbf{Ey} = \mathbf{Ez} = \mathbf{0}. \tag{3}$$

The necessary condition for a *non-degenerate* tensegrity structure is that the force density matrix **E** has rank deficiency of at least four. It should be noted that this is not a sufficient condition for a non-degenerate structure.

A *super stable* structure is always stable irrespective of level of prestress introduced to it; hence, a super stable structure is preferable in designing a tensegrity structure. The authors presented the three necessary and sufficient conditions for super stability of a tensegrity structure [4]:

(a) The force density matrix **E** is positive semi-definite;

(b) The force density matrix **E** has rank deficiency of four; and

(c) The geometry matrix **G** is full-rank.

## 3. Form-finding

This section presents a random strategy for topology generation, briefly introduces the adaptive force density method for finding the feasible force densities, and then presents two optimization problems for searching for the optimal configuration.

### 3.1 Topology Generation

A *ground structure* is defined as the structure of which every pair of nodes are connected by a member, either a strut or a cable. Hence, a ground structure consists of $m(=_2 C_n)$ members in total. To ensure that struts are not connected with each, the number $m^s$ of struts is $n/2$ at most; i.e., $m^s \le n/2$. The typical number of struts is $n/2$, for *n* even, such that every node is connected by a strut and no struts share the same node.

New topologies are generated by removing cables one by one, while all the struts will remain. As there is no 'correct' measure for removing a cable, the cable to be removed is randomly selected: the number $n_i^c$ of cables connected to node *i* is multiplied by a random value $r_i \in [1, 2]$, and the two nodes connected by a cable with the maximum value of $n_i^c r_i$ is then removed.

This random strategy enables us to generate various topologies, and moreover, the numbers of cables connected to each node turn out to be roughly the same.

Once the topology is determined, we are in the position to find the self-equilibrium shape for the structure. The AFDM is divided into two subsequent processes: finding the feasible force densities, and determining the nodal coordinates.

### 3.2 Feasible force densities

The force density matrix **E** has rank deficiency of four if and only if it has four zero eigenvalues. Since **E** is the function of only force densities **q** when topology is determined, eigenvalue analysis is applied to **E** so as to satisfy the non-degeneracy condition: the four smallest eigenvalues of **E** are set to zeros to produce a new **E** having four zero eigenvalues, and **q** is then updated from the new **E** using the least squares method.

The force density matrix calculated from the updated **q** as in Eq.(3) may not satisfy the non-degeneracy condition precisely; hence, it is necessary to iteratively apply eigenvalue analysis to **E**.

It is notable that the first two necessary and sufficient conditions for a super stable structure are satisfied applying the above-mentioned eigenvalue analysis to the force density matrix, and the third condition is related to nodal coordinates determined in the next subsection.

### 3.3 Nodal coordinates

Since a tensegrity structure is a prestressed pin-jointed structure, its shape is described in terms of nodal coordinates, which can be arbitrarily determined as long as the equilibrium equations in Eq.(3) are satisfied. This gives us some limited freedom to search for the desired configuration.

As cables tend to pull the nodes closer while struts push them farther, it would be a good idea to find the self-equilibrium shape by maximizing lengths of cables with limited lengths of struts. Letting $l^c_{\min}$ denote the minimum length of cables, while $\mathbf{l}^s$ denote lengths of struts and $\tilde{\mathbf{l}}^s$ their upper bounds, the following problem is considered:

$$\begin{aligned} \textbf{Opt1}: \quad & \text{Maximize} \quad l^c_{\min} \\ \text{s.t.} \quad & \mathbf{l}^s \le \tilde{\mathbf{l}}^s \\ & \text{Eq.(3)} \end{aligned} \tag{4}$$

Moreover, the structure will degenerate into a two- or even one-dimensional structure if the geometry matrix **G** is rank deficient; i.e., it has zero singular value. The smaller difference among the singular values of **G** may give us a more preferable configuration, hence, we consider the following optimization problem denoting the maximum and minimum singular values of **G** as $\lambda^G_{\max}$ and $\lambda^G_{\min}$:

$$\begin{aligned} \textbf{Opt2}: \quad & \text{Maximize} \quad \lambda^G_{\min} / \lambda^G_{\max} \\ \text{s.t.} \quad & \mathbf{l}^s \le \tilde{\mathbf{l}}^s \\ & \text{Eq.(3)} \end{aligned} \tag{5}$$

## 4. Numerical examples

This section is to present the self-equilibrium shapes of tensegrity structures with different numbers of nodes. Only the structures consisting of $n/2$ struts and $n$ (even) nodes are considered. All struts will have the same force densities, and the initial force densities for starting the adaptive force density method are specified as −1 for struts and +1 for cables. Upper bounds of all struts are set as 1. Both of the optimization problems in Eqs.(4) and (5) are solved using the optimization tool provided by Matlab [5].

The ground structure for the structure with six nodes consists of 15 members, including three struts and twelve cables. Every node is connected by one strut and four cables. Finding the feasible force densities by the AFDM and solving the problem Opt1 determine the super stable structure as shown in Figure.1.(a); struts of the structure intersect with each other at the center. Solving the problem Opt2 gives a similar structure.

Removing the cables one by one generates many different topologies, and some of the stable structures of which struts do not physically intersect with each other are shown in Figure.1.

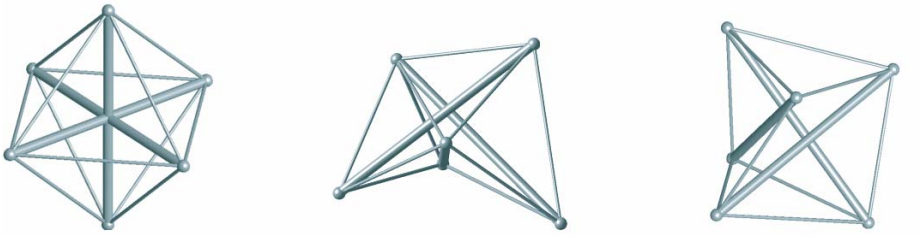

(a) Ground structure, (b) Structure with ten cables, (c) Prismatic structure.

Figure 1: Structures consisting of six nodes and three struts.

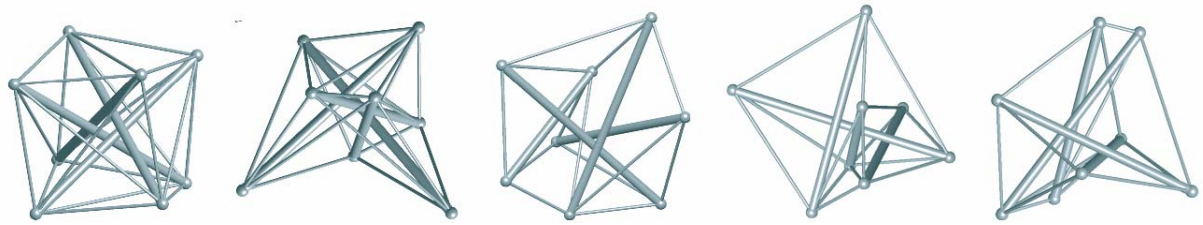

Figure 2: Structures consisting of eight nodes and four struts.

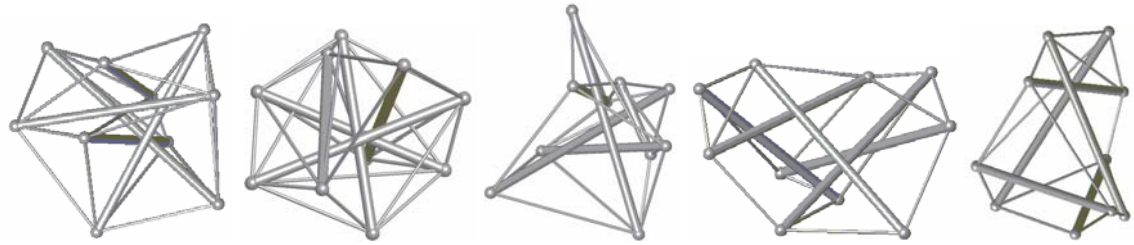

Figure 3: Structures consisting of ten nodes and five struts.

As more complicated cases, some of the structures with eight and ten nodes are shown in Figures.2 and 3, respectively.

## 5. Conclusions

We have investigated topology and self-equilibrium shapes of tensegrity structures in this study. Consecutively removing cables from a ground structure generates many new structures. However, there seems to be no universal rule for generating topology, since super stable structures can be found for every topology although the final configuration might not be the one we expect; e.g., some struts may intersect with others such that these structures cannot be made in practice.

The random strategy adopted in the study for topology generation enables us to investigate the diversity of connectivities of members and nodes, and the adaptive force density method guarantees a super stable structure.

Numerical investigations show that solving problem Opt1 tends to converge to a uniform configuration even different initial solutions are given, while Opt2 tends to generate more elegant configurations expanding fully in the three-dimensional space.

## Acknowledgement

The first author thanks the financial funding as a post-doctoral research fellow from the Japan Society for the Promotion of Science (JSPS).

## References

[1] Fuller, RB. Synergetics, Explorations in the Geometry of Thinking. Collier Macmillan, London, UK, 1975.

[2] Paul C, Lipson H, and Cuevas FJ. 2005. Evolutionary form-finding of tensegrity structures. In *Proceedings of the 2005 Conference on Genetic and Evolutionary Computation*. Beyer H, Ed. ACM, New York, NY, 2005; 3-10.

[3] Zhang, JY, and Ohsaki, M. Adaptive force density method for form-finding problem of tensegrity structures. *International Journal of Solids and Structures* 2006; **43**: 5658-5673.

[4] Zhang, JY,. and Ohsaki, M. Stability Conditions for Tensegrity Structures. *International Journal of Solids and Structures* 2006; **44**: 3875-3886.

[5] Borse GJ. Numerical Method with MATLAB. International Thomson Publishing Inc. 1997.